POLITECNICO DI TORINO

DIMEAS – DEPARTMENT OF MECHANICAL AND AEROSPACE ENGINEERING

MASTER OF SCIENCE DEGREE

IN

AUTOMOTIVE ENGINEERING

Master's degree thesis

Niobium-Alloyed Steels for Automotive Transmission and Powertrain Applications

Supervisor:

Prof. Paolo Matteis

Candidate:

Akshay Arun Patilkulkarni

264883

Academic Year – 2020-2021

Abstract

Niobium-Alloyed Steels for Automotive Transmission and Powertrain Applications

Akshay Arun Patilkulkarni, M.Sc.

Politecnico di Torino

Niobium (Nb), previously called as columbium (Cb), is a ductile, grey colored transition metal that was first reported in 1801 by English chemist Charles Hatchet. Niobium has a large field of applications, among which its role as an alloying element in steels is one of the most important one. Niobium is added in the melt shop during the steel making process in the form of ferrous niobium in order to produce niobium alloyed steels. It is well-known that ferrite stabilizing element that expands the α-field and closed the γ-field of the iron-carbide phase diagram.

The study presents principles of micro-alloying with niobium and titanium and discuss the equilibrium states between austenite and carbides. The effect of micro-alloy of these elements on recrystallization, grain growth, and grain size are discussed. Further, precipitation in ferrite and precipitation strengthening are discussed in the second chapter. Also, hydrogen trapping in carbides and the effect of protection against hydrogen embrittlement is discussed.

The steel components for automotive powertrain and transmission, their properties, strength and manufacturing routes are discussed to understand and improve/eliminate some processes by use of niobium alloy. Heat treatments in use for manufacture of gears, axles, shafts, and flex plates are discussed.

The effect of micro-alloy of niobium in forging steels undergoing controlled cooling is realized. The automotive components undergoing this heat treatment are studied and process route is understood. The microstructure evolution during the heat treatment process due to niobium addition and the effect of micro-alloy is studied, along with improvement of mechanical properties like strength, toughness, and fatigue are seen. Similar study is carried out for forging steels undergoing quenching and tempering, and high temperature carburizing. In the last

chapter, the important effect of hydrogen trapping in niobium micro-alloyed steels is studied. Hydrogen embrittlement and how niobium helps escape prohibited area of ASTM austenite grain size at high temperature carburizing is studied in detail.

Keywords: Niobium, powertrain, transmission, hydrogen trapping, hydrogen embrittlement, controlled cooling, quenching and tempering, high temperature carburizing.

Acknowledgements

I would like to express my earnest appreciation to my thesis supervisor Prof. Paolo Matties for providing me the opportunity to complete this thesis at **CBMM-*Companhia Brasileira de Metalurgia e Mineração, and for all his guidance along the way.***

Special thanks to Dr. Fabio D'Aiuto, the market development manager at CBMM, for following up and help during the development of this thesis. He has always been available for help whenever needed, and taking time to review the thesis, without hesitation, in a very timely manner. Without his assistance the thesis work would have been a much more tough task, and for that I am very thankful.

Last, but not the least, I would like to express my profound gratitude to my family and friends for offering me with unfailing support and continuous encouragement throughout my years of education.

Contents

1 INTRODUCTION 15

1.1 Niobium (Nb) 15

1.2 Properties- physical, chemical, and mechanical 16

1.2.1 Physical properties 16

1.2.2 Chemical properties 16

1.2.3 Mechanical properties 17

1.3 Micro-alloyed steels 17

1.4 Automotive transmission and powertrain 18

1.5 Thesis objective and structure 19

2 PRINCIPLES OF MICROALLOYING 20

2.1 Phase diagrams 20

2.1.1 Iron-Carbon (Fe-C) phase diagram 20

2.1.2 Iron-Carbon-Niobium (Fe-C-Nb) phase diagram 22

2.1.3 Carbon-Iron-Titanium (C-Fe-Ti) phase diagram 23

2.2 Austenite Grain-Size Control in Micro-alloyed Steels 24

2.3 Precipitation in Ferrite 28

2.4 Hydrogen Trapping in Carbides 31

3 STEEL COMPONENTS FOR AUTOMOTIVE POWERTRAIN AND TRANSMISSION 33

3.1 Gear: Manufacturing and Properties 33

3.2 Axle: Manufacturing and Properties 35

3.3 Shaft: Manufacturing and properties 37

3.4 Flex Plate: Manufacturing and properties 38

4 MICROALLOYING OF FORGING STEELS UNDERGOING CONTROLLED COOLING 41

4.1 Types of Forging Steels Undergoing Controlled Cooling 41

4.2 Process Route of Forging Steels 42

4.3 Microstructure Evolution due to Addition of Niobium in Forged Parts undergoing Controlled Cooling 44

4.4 Effect of Micro-alloying Elements on the Microstructure Evolution 49

4.5 Mechanical Properties of Forged Niobium Micro-Alloyed Steels Undergoing Controlled Cooling 50

5 MICRO-ALLOYING OF FORGING STEELS UNDERGOING QUENCHING AND TEMPERING 51

5.1 Types of Forging Steels Undergoing Quenching and Tempering 51

5.2 Process Route of Forged Steels undergoing Quenching and Tempering 52

5.3 Microstructure Evolution due to Addition of Niobium in Forged Parts undergoing Quenching and Tempering 54

..... 54

5.4 Effect of Micro-alloying Elements on the Microstructure Evolution 56

5.5 Mechanical Properties of Forged Niobium Micro-alloyed Steels Undergoing Quenching and Tempering 57

6 MICRO-ALLOYING FOR HIGH TEMPERATURE CARBURIZING 59

6.1 Types of Steels Undergoing High Temperature Carburizing 59

6.2 Process Routes of steels Undergoing High Temperature Carburizing 61

6.3 Microstructure Evolution due to Addition of Niobium in Steels Undergoing High Temperature Carburizing 62

6.4 Effect of Micro-alloying Elements on the Microstructure Evolution 65

6.5 Mechanical Properties of Niobium Micro-alloyed Steels Undergoing High Temperature Carburizing 70

7 MICRO-ALLOYING FOR HYDROGEN TRAPPING IN HIGH-STRENGTH STEELS 72

7.1 Types Steels used for Micro-Alloying for Hydrogen Trapping 72

7.2 Process Route of High-Strength Steels 74

7.3 Microstructure Evolution- Hydrogen Embrittlement and Hydrogen Trapping 76

7.3.1 Fundamentals of Hydrogen Embrittlement 76

7.3.2 Hydrogen Trapping 77

7.4 Effect of Niobium Micro-alloy on Hydrogen Trapping 80

7.5 Mechanical Properties of Niobium Micro-Alloyed Steels after undergoing Hydrogen Trapping Effect 81

8 Conclusion 83

9 References 85

List of Figures

Figure 2-1 Iron-Carbon phase diagram according to [8] 21

Figure 2-3 C-Fe-Nb phase diagram with 0.1 wt.% Nb and 0.02 wt.% Nb [10] 22

Figure 2-4 C-Fe-Ti calculated solubility of TiC in Austenite at 1200ºC [17] 24

Figure 2-5 Solubility product vs Temperature for numerous compounds in austenite [19] ... 26

Figure 2-6Austenite grain coarsening of various micro-alloyed steels [20] 27

Figure 2-7 Austenite grain-coarsening in steels alloyed with different quantity of niobium [20] 28

Figure 3-1Gear production process: Manufacturing stages [30] 34

Figure 3-2 Heat treatment: first-level and Second-level processes [30] 34

Figure 3-3 Axle manufacturing processes [31] 36

Figure 3-4 Driveline for conventional rear wheel drive (RWD) vehicle [34] 37

Figure 3-5 A buckled specimen after the static torque test [35] 38

Figure 3-6 Flex plate manufactured by hot press forming technique [37] 39

Figure 3-7 Flex plate manufacturing process [37] 40

Figure 4-1 Schematic representation of open die forging, closed die forging, roll forging [42] 44

Figure 4-2 Microstructure steel sample forged and a) 30% still air cooled specimen. b) 30% compressed air cooled specimen. c) 30% water spray cooled specimen. d) 50% still air cooled

specimen. e) 50% compressed air cooled specimen. f) 50% water spray cooled specimen [41].Abbreviations are mentioned in Table 4-2 45

Figure 4-3 Representation of low and high magnification scanning electron micrographs of Nb-micro-alloyed steel processed at (a and b) low cooling rate [43] 47

Figure 4-4Representation of low and high magnification scanning electron micrographs of Nb-micro-alloyed steel processed at (a and b) intermediate cooling rate. The figure (b) shows degenerated pearlite [43] 47

Figure 4-5. Representation of low and high magnification scanning electron micrographs of Nb-micro-alloyed steel processed at (a and b) high cooling rate. [43] 48

Figure 5-1 Comparison of processing steps for manufacturing of conventional steels and micro-alloyed steels [49] 53

Figure 5-2Processing steps for manufacturing of non-heat treated bolts using Nb micro-alloyed steels [48] 53

Figure 5-3 Microstructures of steels; upper row: FRT 920ºC, lower row: FRT 820ºC. (a,d) DQ, (b,e) DQ+0.02Nb, (c,f) DQ+0.05Nb [44] 54

Figure 5-4 Transmission electron microscopy (TEM) microstructures of DQ+0.02Nb steel with FRT 820ºC [44] 55

Figure 5-5 Low angle (2.5º-15º, red lines) and high angle(>15º, black lines) boundaries of steels. Upper row: FRT 920ºC, lower row: FRT 820ºC. (a,d) DQ, (b,e) DQ+0.02Nb, (c,f) DQ+0.05Nb. [44] 55

Figure 6-1 New process route for high temperature carburizing [50] 62

Figure 6-2 Former austenite grain size, after blank hardening of 16MnCr5+Nb steel [50] ... 63

Figure 6-3 Grain size distribution of 16MnCr5+Nb steel after forging at 700°C and blank hardening at 1050°C [50] 63

Figure 6-4 Grain size distribution of 16MnCr5+Nb steel after forging at 900°C and blank hardening at 1050°C [50] 64

Figure 6-5Grain size distribution of 16MnCr5+Nb steel after forging at 1250°C and blank hardening at 1050°C [50] 65

Figure 6-6 Calculated nitride and carbide precipitates [50] 65

Figure 6-7 Solubility behavior of NbC and Nb(C,N) as function of temperature and influence of other alloying elements [62] 67

Figure 6-8 Solubility behavior of NbC and Nb(C,N) as function of temperature and influence of other alloying elements [62] 67

Figure 6-9 Effect of case hardening temperature on grain size. Austenizing for 2h 47min and oil quench. [50] 68

Figure 6-10 Grain growth tests of microalloyed melts of a MoCr steel in the FP annealed pre condition after 950°C and 25 hours holding time [64] 69

Figure 6-11Grain growth studies of the micro-alloyed melts of a MoCr steel in annealed pre-condition after 1050°C and 15 hours holding time [64] 70

Figure 7-1 a) Schematic representation of heat treatment procedures [70] 74

Figure 7-2 Thermo mechanical treatment schedule for production of press hardening steel [71] 75

Figure 7-3 Hydrogen trapping by the addition of Niobium [1] 77

Figure 7-4 Fracture surfaces for the specimens with different content of Nb, a) 22MnB5, b) 22MnB5 + 0.027%Nb, c) 22MnB5 + 0.049%Nb [73] 78

Figure 7-5 Stress-Strain curves of tested steels electrochemically charged at various contents of Nb [73] 79

Figure 7-6 Engineering stress vs strain curves of the three PHS [73] 81

Figure 7-7 Tensile strength of investigated steel with various niobium content a) hot rolled steels b) press hardening steels [73] 81

List of Tables

Table 1-1Physical properties of Niobium [3] 16

Table 1-2 Mechanical properties of Niobium [3] 17

Table 2-1 Temperature dependence of solubility products (K) containing Niobium for Carbide, Nitride, and Carbonitride in austenite [18] 27

Table 2-2 Characteristics of niobium carbonitride precipitate in hot rolled 0.06% C, 0.6% Mn, 0.006% N steel with addition of 0.02% Nb, 0.06% Ti [23] 31

Table 3-1Fatigue life of gears with different torque loads [30] 35

Table 3-2 Detailed chemical composition of SK5 steel [37] 39

Table 4-1 Chemical composition of various steels [38] [39] [40] [41] 42

Table 4-2 Microstructure of examined specimen in as-forged condition [41] 46

Table 4-3 Microstructural characteristics of Nb micro-alloyed steels [43] 49

Table 4-4 Representation of room temperature tensile and impact properties of Nb micro-alloyed steels [43] 50

Table 5-2 Chemical composition of forged steels undergoing quenching and tempering [48] [49] 52

Table 5-3 Tensile properties, Charpy V impact properties of forged steels ;Agt is the total uniform elongation (elastic +plastic) as defined in ISO 6892-1:2009 [44] 57

Table 6-1Chemical composition of metals undergoing high temperature carburizing [56] [50] [55] [57] [58] 60

Table 6-2 Comparison of required time for several process periods [50] 61

Table 6-3 Mechanical properties at room temperature of 20CrMo5 mod. Steel [64] 71

Table 7-1 Chemical composition of steels [68] [69] [70] 73

Table 7-2 Tensile properties of investigated steels [73] 82

List of Equations

Equation 1 20

Equation 2 20

Equation 3 21

Equation 4 23

Equation 5 [10] 23

Equation 6 25

Equation 7 25

Equation 8 25

Equation 9 76

Equation 10 76

Equation 11Anodic dissolution of Fe (Volmer reaction) 76

Equation 12 Recombination od absorbed H (Tafel reaction) 77

Equation 13: Absorption of H_{ad} 77

Objective

This work is aimed at providing a bibliographic research for niobium micro-alloyed steels for automotive transmission and powertrain applications. The thesis also sheds light on the added value corresponding to addition of niobium in terms of mechanical and metallurgical mechanisms. Applications considering the main trends of the future in what concerns the niobium addition as a micro-alloying elements in stees.

1 INTRODUCTION

1.1 Niobium (Nb)

[1] [2] Niobium (Nb) is an important element in today's and future world. Niobium was discovered by British mineralogist and analytical chemist Charles Hatchett in 1801. The name derives from Greek Goddess Niobe, daughter of Dione and Tantalus. Niobium, formerly known as Columbium (Cb) is a rare, soft, ductile, malleable, grey-white metal. It has an atomic number 41 in the periodic table and an atomic mass of 92.90638 u. It falls in the category of transition metals, that is, it occupies central block in the periodic table . Like other transition metals, chemically, Niobium has a variable valency and a strong tendency to form coordination compounds .Some notable physical properties are, Niobium has a high melting point of 2,477 ºC and a density of 8.4 $g.cm^{-3}$ at 20 ºC. Pure Niobium has a Mohs hardness rating similar to that of Titanium (Ti) and ductility similar to Iron (Fe). Because of such chemical and physical properties, Niobium has attracted several researchers and mineralogists to do further study on it.

Around 85 resources of Niobium have been found around the world. Brazil is the leading producer of Niobium with more than 85% of production, followed by Canada which produce over 10%. Rest of the world produces just about 2% of Niobium. Brazil holds about 98% of the World's Niobium, making it Niobium capital of the world. The country has 842,460,000 tons of Niobium across several reserves. The largest deposits are found in the states of Minas Gerais, Goias and Amazonas. Companhia Brasileira de Metalurgia e Mineração (CBMM) is the leading manufacturer of Niobium. CBMM is a Brazilian company that specialises in processing and technology of Niobium. Founded in 1955 with its headquarters in Araxá, State of Minas Gerais, Brazil, CBMM is a fully integrated company that produces Niobium from mine to final products. CBMM is segment leader in the industry present across South America, North America, Europe and Asia. It has its mine reserve in Araxá, where the element occurs in its oxidised form.

1.2 Properties- physical, chemical, and mechanical

[3]Niobium occupies 33rd position in the order of abundance in nature and is present in Earth's crust at 24 µg/g. It occurs more commonly than other ores like Cobalt, Molybdenum, and Tantalum.

1.2.1 Physical properties

[3]Niobium is a refractory metal, that is it exhibits extraordinary resistance to heat and wear ,and has a high melting point (2,468 ± 10°C). The table below shows some other important physical properties of Niobium:

Table 1-1Physical properties of Niobium [3]

Properties	Values
Density at 20 °C	8.57 g/cm^3
Crystal structure	Body-centred-cube (BCC)
Melting point	2648 ± 10 °C
Boiling point	4927 °C
Specific heat	0.26 kJ kg^{-1} K^{-1}
Linear coefficient of thermal expansion	6.892 x 10^{-6} K^{-1}
Thermal conductivity at 0°C	53.7 Wm^{-1} K^{-1}
Electric conductivity	6.58 x 10^6 AV^{-1} m^{-1}
Magnetism (Natural state)	Paramagnetic
Superconductivity, T_c	9.13 K

1.2.2 Chemical properties

[3] [2]About the chemical properties of Niobium, it is a transition metal located in the middle of periodic table in group V, period 5. Other alloying elements such as Vanadium, Molybdenum, and Manganese are also located nearby. In the air, Niobium is a very a very stable element and has a bluish tinge (if exposure to air is prolonged). It has low affinity to Oxygen that lasts up to 200°C, this property of Niobium is what makes it an important alloying

element. On the other hand, Niobium has higher affinity for Carbon and Nitrogen as compared to Oxygen, which is important in application to steel.

Niobium has a tendency to form oxides, hydrides, nitrides, and carbides. Niobium has a few oxidation state, of which +5 is the most stable one. Niobium after mining, occurs in Nb_2O_5 oxide state from which several products are obtained.

1.2.3 Mechanical properties

[3]The mechanical properties are influenced mainly by purity of the metal, the method of production and also on the mechanical treatments it undergoes. Since Niobium is a micro-alloying element, addition of Niobium even in small amounts increases hardness and strength. In the table below, some of the important mechanical properties of annealed Niobium have been mentioned:

Table 1-2 Mechanical properties of Niobium [3]

Properties	Values
Yield strength	105 MPa
Ultimate tensile strength	195 MPa
Poisson's ratio	0.38
Elongation	30% +
Reduction in area	80% +
Hardness	60 HV
Elastic modulus (Tension)	103 GPa
Elastic modulus (shear)	17.5 GPa
Recrystallization temperature	800-1000 °C

The mechanical properties of cold worked Niobium are considerably different. The ultimate tensile strength is 585 MPa (about 3 times higher than annealed Nb), while elongation is reduced to 5%, and Hardness is increased to 150 HV (2.5 times higher than annealed Nb).

1.3 Micro-alloyed steels

Micro alloying is the process of alloying materials with small amount (0.05% to 0.15%) of elements to refine grain structure or facilitate precipitation hardening. Steel is micro alloyed

with elements like Niobium, Vanadium, Titanium, Molybdenum, Zirconium, boron and other rare-Earth materials.

Special Bar Quality (SBQ) steel is a class of steel product engineered for tough applications such as bearings, crankshafts, gears etc. Special Bar Quality (SBQ) steels display extraordinary stress resilience and associated metal fatigue tolerance. These are apt for versatile applications where high efficiency are highly demanded. The properties are achieved through thermal treatment process.

1.4 Automotive transmission and powertrain

[4] [5]Automotive transmission is a power transmission system installed in a automobile, to match the torque available from engine to the needs of the wheels, depending on the road conditions, driver's will and other factors. The transmission helps us to determine numerous vehicle functions such as consumption of fuel, emissions, vehicle dynamics etc. At present the most commonly used transmissions are manual (5 speed or 6 speed), continuously variable transmission (CVT), and automatic transmission (AT). A dual-clutch transmission (DCT) is mostly employed in high performance sports cars where gear change needs to be lightning fast.

Powertrain in an automobile is also a power transmission system that includes an internal combustion (IC) engine (mostly a reciprocating engine in modern cars), and a gearbox, that converts torque of engine to torque necessary for vehicle traction.

Steel is one of the most used material in automotive industry. However, plain carbon steel is now replaced by high strength steels (HSS) and high strength low-alloy steels (HSLA) on account of their higher strength. Also, the use of aluminium alloys has also increased from 2% of curb weight in 1970s to almost 8.8% in 2010s and is predicted to reach about 10% or higher in 2020s. Much of this aluminium alloy is used in engine cylinder blocks, transmission components, suspension parts, and body parts.

1.5 Thesis objective and structure

This thesis investigates in, to provide an overview of applications of Niobium as a micro-alloy in steels for automotive transmission and powertrain. The thesis also discuss about enhancement in properties of steels by using Niobium as a micro-alloying agent.

The report of thesis is structured to first give an insight about principles of micro-alloying. Later it explores about the steel components used for automotive transmission and powertrains. Then ventures into micro-alloying of forging steels undergoing controlled cooling. In this chapter, details about the type of steels used, processes the steel undergoes and micro structure evolution during the process are discussed. A similar sub-structure is used for next chapters. The thesis is followed up by micro-alloying of forging steels undergoing quenching and tempering process, high temperature carburizing, and hydrogen trapping in steels. The thesis ends with conclusion of the thesis topic and last chapter as references used during writing of the report.

During the thesis work, no new additional experiments have been conducted, a literature review has been carried out and works of several prominent authors are presented. Comparison has been made among several journals and papers, in order to understand the arguments.

2 PRINCIPLES OF MICROALLOYING

2.1 Phase diagrams

2.1.1 Iron-Carbon (Fe-C) phase diagram

[6] In order to understand the principles of microalloying steels with Niobium and other elements, first it is necessary to understand the basic Iron-Carbon (Fe-C) phase diagram. The phase diagram is a function of percentage of carbon (%) vs temperature (ºC), that shows regions of existence and composition of various equilibrium phases of Iron-Carbon system. For any system, there is only one equilibrium state at a specific temperature, whereas there are many non-equilibrium phases and non-equilibrium states. Every Iron-Carbon phase diagram stops at Iron Carbide (Fe_3C), that is an inter-metallic compound with weight percentage of 6.67. Beyond 6.67 Carbon percentage the alloy becomes too brittle and does not have much engineering applications.

[7] Some important phases and their transformations have been discussed below. Pure iron when heated experiences two changes in crystal structure before it melts. First, at room temperature, iron is present in its stable form, known as Ferrite (α-iron). α-Ferrite has a Body Centered Cube (BCC) crystal structure. Secondly, at 912ºC Ferrite experiences polymorphic transformation to form Face Centred Cube (FCC) Austenite (γ-iron). This Austenite persists till 1394ºC, at which FCC Austenite reverts back to BCC phase. This BCC phase ferrite is called δ-Ferrite. This δ-Ferrite finally melts at 1538ºC. In Figure 2-1 Iron-Carbon phase diagram according to has been shown. The diagram consists of three invariant reactions namely, peritectic reaction, eutectic reaction, and eutectoid reaction. Peritectic reaction occurs at 1493 ºC, that transforms δ-Ferrite and Liquid into Austenite (γ) upon cooling.

$$\delta Ferrite + Liquid \xrightarrow{1493^{o}C\,,cooling} Austenite\ (\gamma)$$

Equation 1

Eutectic reaction occurs at lower temperature, at 1150 ºC upon cooling, Liquid transforms into Austenite (γ) and Cementite.

$$Liquid \xrightarrow{1150^{o}C\,,cooling} Austenite\ (\gamma) + Cementite$$

Equation 2

Third reaction occurs at a low temperature, at 725 ºC upon cooling, Austenite (γ) transforms into α-Ferrite and Cementite.

$$Austenite\ (\gamma) \xrightarrow{725^{o}C\ ,cooling} \alpha Ferrite + Cementite$$

Equation 3

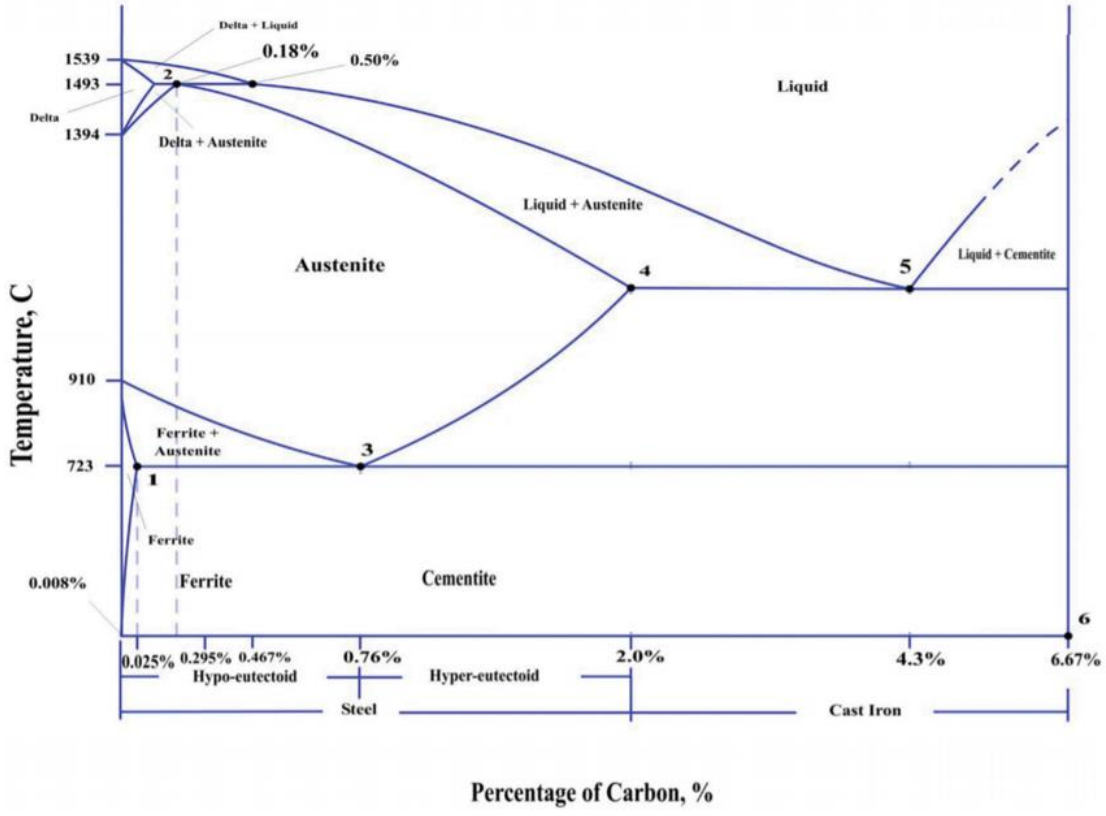

Figure 2-1 Iron-Carbon phase diagram according to [8]

At 4.3 percentage of Carbon and 1150 ºC, the lowest melting point can be seen in the whole alloy system. This is beneficial for casting process, as casting alloys have higher carbon content and the lower melting point makes casting process possible at lower temperatures. It is evident from Figure 2-1 Iron-Carbon phase diagram according to that steels have higher melting point. Also, eutectoid reaction is one of the most important reaction from alloying point of view as this reaction gives control on micro-structure of steel through various heat treatment processes. When the percentage of carbon is less than 2% in iron, it leads to formation of steel alloy. Above 2%-6.67% percentage of carbon in iron, there is formation of cast iron.

2.1.2 Iron-Carbon-Niobium (Fe-C-Nb) phase diagram

[9] [10] [11] [12]. [10] reported that, in NbC system, Fe and Nb atoms are distributed in FCC sites, with octahedral voids occupied by C atoms. Therefore, the equilibrium between Austenite (γ) and NbC may be treated as immiscible gap between these two phases. When a strong negative interaction parameter between Nb and C in Austenite (γ) is introduced, an increase in solubility of Nb is evident with increasing C in Austenite (γ) at higher C contents. [13] also noted that, there is a strong interaction between Nb and C in Austenite (γ). This was accountable for the increase in Nb solubility with increasing C wt.% at higher C levels.

A vertical along Fe-NbC joint was calculated by [11]. The eutectic point is found at 2.6% Nb (4.3wt.%) and at 1464 ºC. [11] also calculated couple of other vertical sections for Fe rich alloys at 0.02 wt.% Nb and 0.1 wt.% Nb. The Figure 2-2 C-Fe-Nb phase diagram with 0.1 wt.% Nb and 0.02 wt.% Nb compares the results with the results of [10].

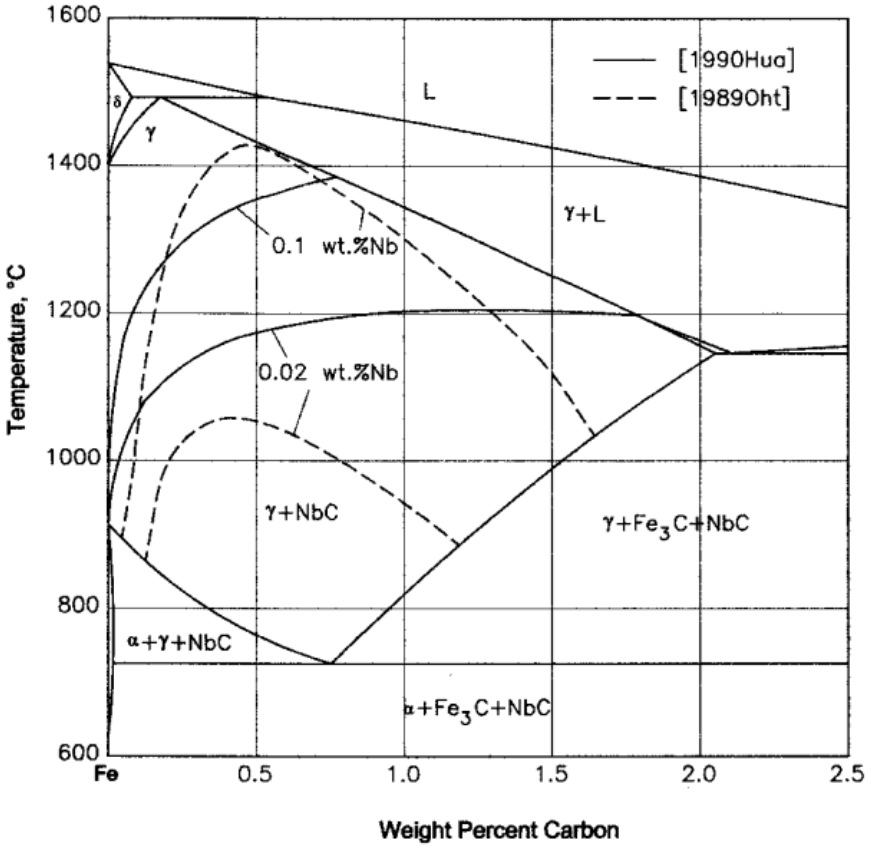

Figure 2-2 C-Fe-Nb phase diagram with 0.1 wt.% Nb and 0.02 wt.% Nb [10]

There have been several studies in the past that have reported on solubility of NbC in Austenite. [14] which was reviewed by [15] used sealed capsule method to determine solubility limit. In this, the binary Fe-C system and Fe-Nb alloys are sealed in same thick walled quartz tube without any physical contact. During annealing process, the vapour phase of Carbon is transferred between solid samples. After equilibrium is attained, with the aid of known activity-composition relationships for Fe-C alloys, carbon activity in ternary alloys system is calculated. Further, iso-activity cures are constructed and with the help of breaks in these curves, the phase boundary corresponding to solubility limit is determined. [14] in the journal, derived an empirical equation for solubility limit by assuming $NbC_{0.87}$ composition for the C-deficient monocarbide.

$$log_{10}[wt.\%Nb][wt.\%C]^{0.87} = -\frac{7920}{T(K)} + 3.4$$

Equation 4

The Equation 4 is valid for a temperature range from 1000 ºC to 1250 ºC with carbon up to 0.4 wt.%. Again by using Equation 4, the γ/γ+ NbC phase boundary corresponding to solubility limit may be calculated. [16] reported new solubility measurements for alloys containing up to 1 wt,% C and in temperature range of 1000 ºC and 1200 ºC, by the use of diffusion couple technique. It was also discovered that as the C content increased beyond 0.5 wt.%, the solubility limit of Nb increased. This indicate withdrawal from hyperbolic behaviour and the empirical solubility product has an additional carbon dependent term. The new equation is presented below:

$$log_{10}[wt.\%Nb][wt.\%C] = -5600/\ T(K) + 1.74 + wt.\%C[1380/T(K)-0.027]$$

Equation 5 [10]

The phase boundary corresponding to solubility limit is calculated using this equation as well.

2.1.3 Carbon-Iron-Titanium (C-Fe-Ti) phase diagram

A thorough thermodynamic assessment of C-Fe-Ti ternary system was carried out by [17]. The liquid phase was modelled as a substitutional solution of Fe, Ti, C. And the solid solution phases namely Hexagonal Closed Packed (HCP), Face Centred Cubic (FCC) and Body Centred Cubic (BCC) were defined by a two sub-lattice model (Fe,Ti)(C,Va), where Va stands for

vacancy. The FCC solid solution austenite and NaCl FCC phase TiC were also defined by identical model. It is also noted that the austenite-TiC two phase is a miscibility gap. In order to interpret for the departure from hyperbolic performance of the solubility of TiC in austenite and to evade any substantial dissolution of Fe in TiC, [17] selected reciprocating interaction parameters for the interaction amongst C and the metal atoms in austenite. The parameters are connected in such a means that, there is a negative influence to the Gibbs energy at the Fe corner and a positive influence at the TiC end. Solubility of C in Fe_2Ti and FeTi was not considered. Cementite (Fe_3C) was defined as a line compound with no solubility of Ti. The diagram below represents thermodynamic assessment of the C-Fe-Ti ternary system.

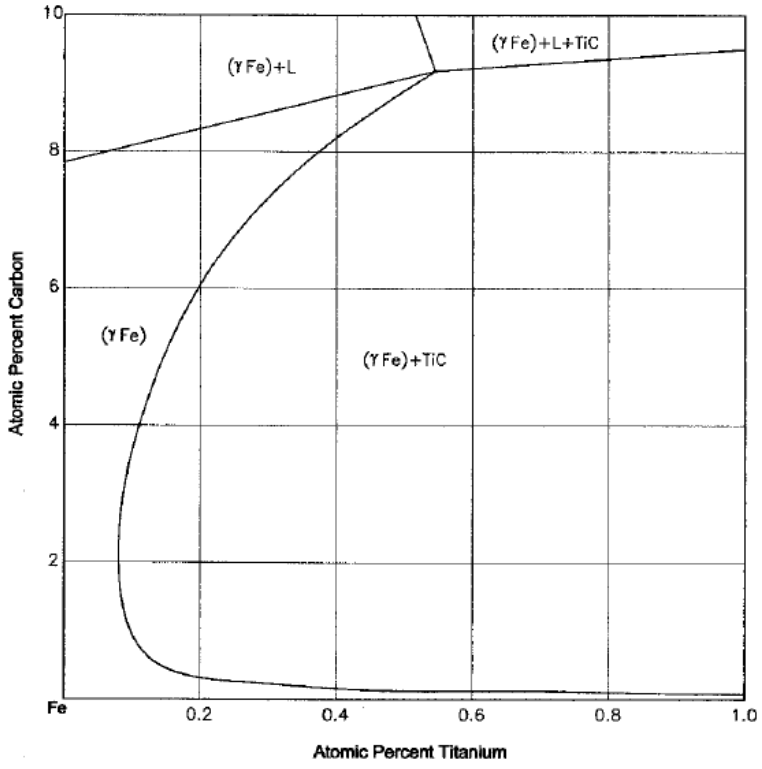

Figure 2-3 C-Fe-Ti calculated solubility of TiC in Austenite at 1200°C [17]

2.2 Austenite Grain-Size Control in Micro-alloyed Steels

Addition of elements such as niobium, vanadium, molybdenum, and titanium, in small amounts in the order of 0.05-0.15% to steel provides a significant cost-effective approach in controlling grain-size and strengthening of steels. The term micro-alloy is used to such metals in contrast with other elements that needs to be added up to more than a few percentage. The principle for micro-alloying using elements niobium, vanadium, and titanium for austenite grain-size

control, is same as to addition of aluminium for austenitic grain-size control. [18] Aluminium addition in the order of 0.02 to 0.04%, to improve grain-size, qualify as a micro-alloying agent, but aluminium alloyed steels are never referred as micro-alloyed steels. This is due to the fact that aluminium is generally added to low alloy steels that contain substantial amount of other alloying elements like chromium, nickel etc. Whereas steels that are micro-alloyed with elements such as niobium, vanadium, titanium etc do not require such additions.

The evaluation of precipitation and grain-size control by micro-alloying is generally based on reactions between substantial elements X which includes niobium, vanadium, aluminium etc. The interstitial elements, Y, includes carbon and/or nitrogen, in austenite to form a compound known as XY_n :

$$\underline{X}+n\underline{Y} = XY_n$$

Equation 6

The underlined X and Y indicate that the elements are in solution phase in austenite. Most often, the factor n is unity, as in the case of AlN. The solubility product or the equilibrium constant, K, for a certain reaction is specified as:

$$K=[X][Y]^n$$

Equation 7

In Equation 7, X and Y represent the wt.% of elements X and Y which are dissolved in austenite. The dependence of temperature of solubility product is given as:

$$\log[X][Y]^n = -A/T + B$$

Equation 8

Where A and B represent constants that may be estimated from free-energy data or are determined from experiments, and it has to be noted that the temperature, T, is in Kelvin.

The Figure 2-4 Solubility product vs Temperature for numerous compounds in austenite , demonstrates solubility product as a function of temperature for several reactions in austenite. The curves that formed from numerous combination of elements, are recognized by compounds, carbides, nitrides, and carbonitride. As the solubility product goes higher, solubility of the reacting elements also goes higher. Also, it may be noted from the figure that,

all curves decrease with a decrease in temperature. This indicates that in due course, austenite gets supersaturated with the elements and precipitation occurs.

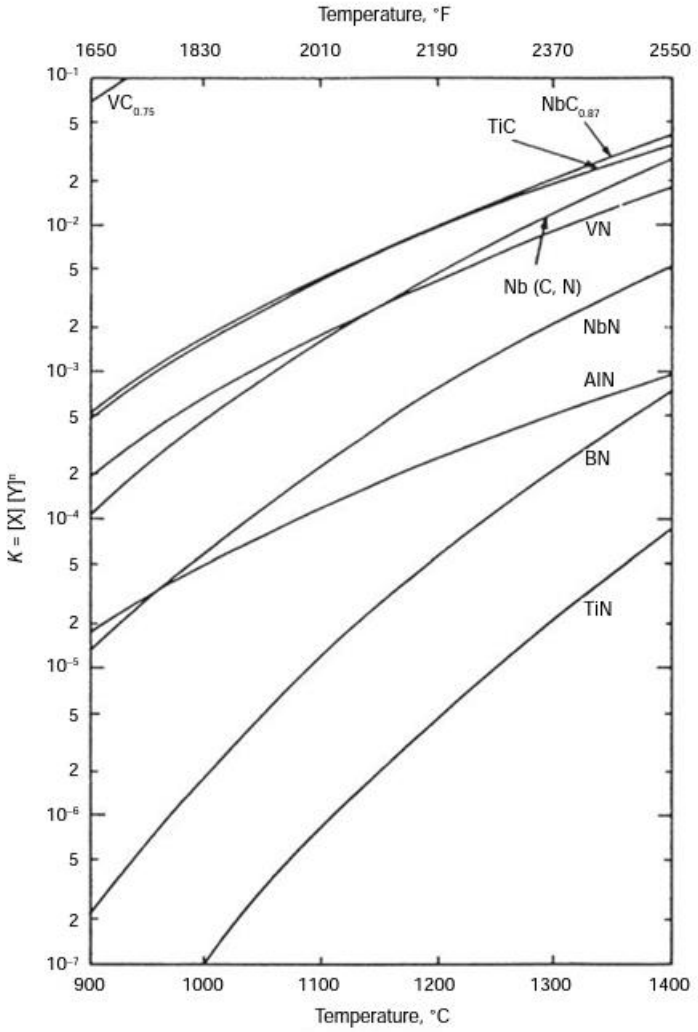

Figure 2-4 Solubility product vs Temperature for numerous compounds in austenite [19]

Moreover, aluminium, boron, and titanium have relatively lower solubility and readily forms nitride precipitates at low concentrations in austenite. Vanadium and niobium compounds have comparatively high solubility in contrast to above mentioned elements. In Table 2-1 Temperature dependence of solubility products (K) containing Niobium for Carbide, Nitride, and Carbonitride in austenite has been listed below.

The austenitic grain growth is retarded with dispersion of fine particles of the micro-alloying elements. At high temperatures, when the particle is more stable, the grain growth process is more efficiently retarded. From Figure 2-5Austenite grain coarsening of various micro-alloyed

steels can be seen. The C-Mn curve that represents plain carbon steel with zero particle dispersion, as temperature increases grain size increases continuously. Whereas, all other elements demonstrate suppression of grain growth at low austenite temperatures, according to their temperature dependent solubility. Another element that may be noted is vanadium, it has the highest solubility, and hence, vanadium carbonitride precipitates dissolve at lowest temperature among all others. This causes discontinuous grain coarsening at lower temperatures as compared with steels alloyed with different elements. Titanium nitride on the other side has remarkable stability, and hence, there is negligible or no grain coarsening effect even at higher temperatures of hot work and forging. At higher temperatures of 1150 ºC and above, niobium has second highest stability after titanium nitride. At 1200 ºC, only niobium and titanium nitride offer average grain-size of less than 150 µm. This demonstrates the high stability of the two elements.

The quantity of micro-alloying elements govern when the solubility for any given element is exceeded.

Table 2-1 Temperature dependence of solubility products (K) containing Niobium for Carbide, Nitride, and Carbonitride in austenite [18]

Solubility products	log K
[%Nb][%N]	-10,150/T + 3.79
$[\%Nb][\%C]^{0.7}[\%N]^{0.2}$	-9,450/T + 4.12
$[\%Nb][\%C]^{0.87}$	-7020/T + 2.81

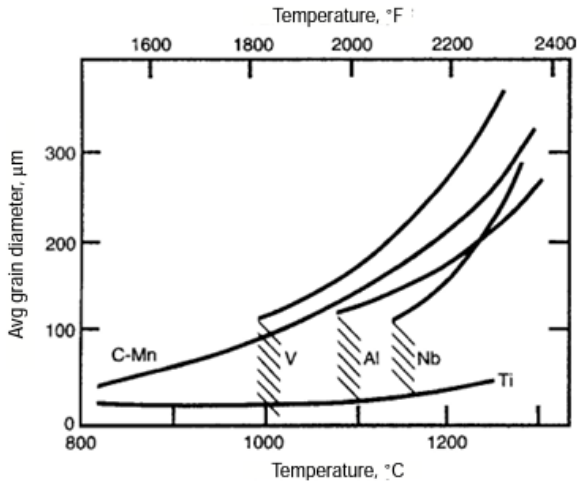

Figure 2-5Austenite grain coarsening of various micro-alloyed steels [20]

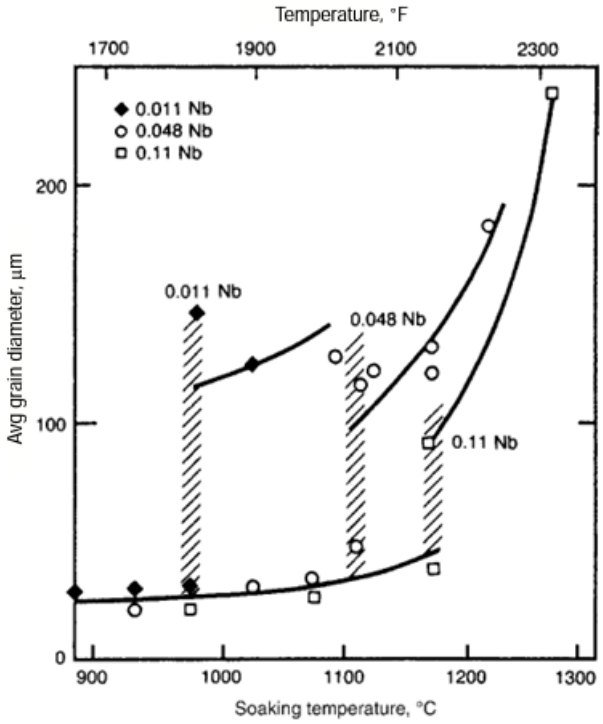

Figure 2-6 Austenite grain-coarsening in steels alloyed with different quantity of niobium [20]

[18] [21] In Figure 2-6 Austenite grain-coarsening in steels alloyed with different quantity of niobium can be seen. At higher concentration of niobium, the higher is the temperature at which solubility is surpassed. That is, more amount of niobium can be dissolved in austenite. As a consequence, as the content of niobium increases, the grain is suppressed more effectively at higher temperatures in comparison with steels with lower concentrations of niobium.

2.3 Precipitation in Ferrite

[22] The precipitation of Nb in ferrite is widely employed in steels. There are two main applications, firstly for low solute content Interstitial Free steels (IF steels), by the removal of C and N atoms off the solid solution, the drawability is improved by precipitation of NbC. Secondly, for high solute contents (High Strength Low Alloy steels), precipitation hardening is provided by the precipitation of Nb carbonitrides. In spite of its high demand for steel industry, there is incomplete characterization of NbC precipitation in ferrite, both qualitatively and quantitatively.

[23] The process for precipitation in ferrite is analogous to niobium carbonitride formation in austenite. Upon cooling down to rolling temperature, there is formation of niobium

supersaturated austenitic matrix. Niobium carbide can nucleate homogeneously inside the matrix, or most probably, heterogeneously on dislocations, phase boundaries, sub-grain, grain together with other precipitates like aluminium, titanium nitrides. While kinetics delay the static formation of niobium carbide in undeformed austenite up to few minutes, the deformation can initiate impulsive precipitation. In steel characterized by 0.03 % Nb, and 0.05 % C + 0.01% N, the static creation of niobium carbide has the highest nucleation rate after about 100 seconds at around 950 ºC. Nevertheless, the dynamic nucleation initiates without a long incubation period, and the highest nucleate rate sifts down to about 900 ºC.

Thermodynamics of niobium carbonitride precipitation in ferrite has been discussed in this section. The niobium in solid solution phase at finish rolling temperature is present for the formation of fine niobium carbonitride precipitate in ferrite. As they are of proportionate size, they provide an increase in strength via precipitation hardening. The equilibrium solubility in ferrite may be presumed from solubility products effective for austenite. It is observed that for a steel characterized by 0.03% Nb, 0.05% C, and 0.01% N, about 1 ppm Nb will remain in solid solution phase when thermal equilibrium is achieved at 800 ºC.

In the precipitation kinetics during cooling, the solute niobium, that has not been precipitated during austenite processing, may form niobium carbides in the interphase between ferrite and austenite, as well as inside ferrite grains. An atomic Monte Carlo method was proposed for simulation of homogeneous nucleation and growth of niobium carbide precipitates in ferrite. The model uses vacancy diffusion mechanism for niobium and iron atoms, and for the carbon atoms interstitial mechanism is employed. The mechanism displayed unexpected development of transient iron carbide clusters in advance to NbC precipitation for particular temperature and concentrations. This formation path can be described by competition amongst the driving force for NbC precipitation and fast diffusion of interstitial carbon. This interstitial carbon balances the weak driving force for iron carbide precipitation at a temperature range of 500 ºC to 700 ºC. The traditional mechanism to determine the effect of precipitation in ferrite was solution treatment of niobium containing steel . This was followed by quenching, so as to avoid any precipitation in austenite. The treated samples were annealed isothermally at different temperatures in ferrite region and hardness that was established was measured over the annealing time.

Niobium carbide precipitation in ferrite region is seen in niobium containing steels that are subjected to laboratory and industrial thermal and thermo-mechanical processes. The finish rolling and cooling conditions determine the probability of formation of niobium carbide precipitates in ferrite or in austenite-ferrite interphase during phase transformation. Precipitates that are formed in ferrite region are characteristically seen after slow cooling from a finish rolling temperature of around 900 ºC. And isothermal holding at coiling temperatures at 600 ºC or more or after high temperature coiling over 680 ºC and coil cooling at a rate of 0.5 ºC/min [23]. There is a high chance of formation of genuine ferrite precipitates, when the rate of cooling is high, in the order of 50 ºC/sec, and isothermal holding temperature is about 600 ºC. Although the air cooling encourages the formation of interphase precipitates. The studies investigating industrial processing cooling rates higher than 10 ºC/sec from finished rolling temperature is characteristic coiling temperatures in the range of 550 ºC to 650 ºC did not display ferrite precipitation, when coiling cooling rates of 0.5 ºC/min or higher were used.

Discussion about the effect of precipitation in ferrite has been made in this section. It is identified from various materials systems, that a high enough density of coherent precipitates may encourage a significant strengthening effect, to which several different dislocation or particle interaction mechanism might contribute. Therefore, it is not certain whether coherent precipitates contribute significantly to strengthen micro-alloyed steels or not. The increase of strength by precipitation hardening of micro-alloyed hot rolled steels is affected by the distribution of niobium carbonitride precipitates, volume, and size. With the help of Ashby-Orowan model, it is possible to evaluate the effect of hardening from niobium in solid solution. The process comprises of a quench hardening and ageing treatment. Carbon in solid solution is supposed to be trapped completely by defects. And the ferrite grains do not alter in size during the aging process. As a consequence, the effects can not contribute to hardness variation.

Table 2-2 below shows some characteristics of niobium carbonitride precipitate in a particular steel with 0.02% niobium and 0.06% titanium.

Table 2-2 Characteristics of niobium carbonitride precipitate in hot rolled 0.06% C, 0.6% Mn, 0.006% N steel with addition of 0.02% Nb, 0.06% Ti [23]

Type of precipitate	Statistics of observations	Mean size of particles (nm)	Particle volume fraction	Percentage of micro-alloy addition
Eutectic carbonitride	>300 particles in ~10 μm^2 area	>1000	5.6×10^{-4}	42.7
Undissolved carbonitride	26 particles in ~500μm^2 area	67	0.8×10^{-4}	6.1
Fine carbonitride after rolling	~ 2500 particles in ~10μm^2 area	6.8	3.6×10^{-4}	27.5
			TOTAL	76.3%

2.4 Hydrogen Trapping in Carbides

[24] Even though the phenomenon of hydrogen embrittlement was first acknowledged over hundred years ago, hydrogen embrittlement still remains a mysterious industrial challenge. High-strength steels are in particularly vulnerable to early fracture and toughness reduced in the presence of hydrogen. This confines the manufacturing routings and application in industries. A good example is automotive industry, that is trying to increase use of high-strength steels to increase fuel efficiency by reduction of weight, while still being able to meet strength requirements. [25] In order to reduce the quantity of diffusible hydrogen in the steels, and therefore reduce vulnerability towards hydrogen damage, the introduction of carbides as hydrogen trapping sites is a well-known approach. Next to vanadium, and titanium, niobium is a good carbide forming alloy element. Nevertheless, the interaction amongst NbC precipitates and hydrogen has been hardly assessed in detail.

Formerly, based on hydrogen permeation experiments, the outcomes of Gehrmann had claimed, that NbN and NbC precipitates were deep hydrogen traps [26]. NbC precipitates are considered to contain numerous hydrogen trapping sites with different activation energies, for instance precipitate-ferrite interface. The coherency strain area adjacent to the precipitates and crystallographic defects inside the precipitate. The hydrogen trapping capacity of NbC is claimed to be higher than that for VC, TiC precipitates.

[24] A reasonable claim is that, the hydrogen trapping is due to affinity amongst hydrogen and carbon atoms. Although, a study presented that carbon atoms in lattice defects have only a weak impact on hydrogen trapping [27]. Other models have effectively predicted the presence of hydrogen trapped at dislocations in body centred cube (BCC structure) lattice. Hence, we can consider that the observed hydrogen is associated directly the existence of lattice defects, rather than the consequence of attraction by segregated carbon atoms [28].

Therefore we can conclude that information about hydrogen trapping at incoherent interfaces offers a path for the design of alloys in which hydrogen embrittlement is prevented or delayed. Further discussion on this topic has been made in chapter 7.

3 STEEL COMPONENTS FOR AUTOMOTIVE POWERTRAIN AND TRANSMISSION

[29] Reduction of weight of vehicle through material replacement is one of the vital aspect in overall strategy for improving fuel economy and emission control. Although the prime material in today's vehicles in carbon steel, there is a great interest in replacing them with advanced steels with high strength, with titanium, niobium alloys. This chapter discusses about various parts of automotive powertrain and transmission, their properties and required strength, and some common heat treatments, surface treatments in use to manufacture these parts.

3.1 Gear: Manufacturing and Properties

[30] Gear transmission is the most significant and extensively used transmission system in mechanical transmission. The performance of gears directly affect the performance of the whole transmission system. Specifically, long life precision gears are extensively employed in mechanical transmission systems with high reliability requirements, like wind turbine gear boxes, and aero engines. Along with continuous development of technology, the requirements of long-life precision gears are also increasing. There are several manufacturing processes that impact the performance of gears, but until now, limited researchers have performed a complete optimization analysis.

Here, 20CrMnTi gear production process by a gear manufacturer is considered for research and analysis. Owing to severe service conditions and high technical requirements of gears, carburizing and grinding processes are used for manufacturing them. The production route of gears is divided into seven main stages in accordance with production sequence, which are structural dimension design stage, material selection phase, forging phase, roughing phase, heat treatment phase, finish machining phase, and testing phase. The heat treatment stage consists of 4 second-level processes, namely, normalizing process, carburizing process, quenching process, tempering process. Similarly, there are 20 second-level processes and 88 first-level processes involved in these seven stages, but heat treatment stage is of relevance to this thesis. The main manufacturing stages has been presented in Figure 3-1. The second-level and first-level processes heat treatment stage has been presented in Figure 3-2 Heat treatment: first-level and Second-level processes.

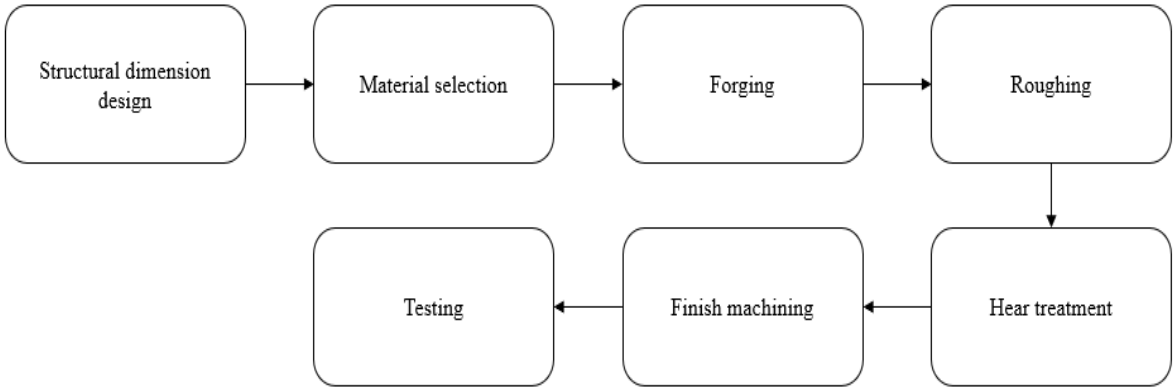

Figure 3-1Gear production process: Manufacturing stages [30]

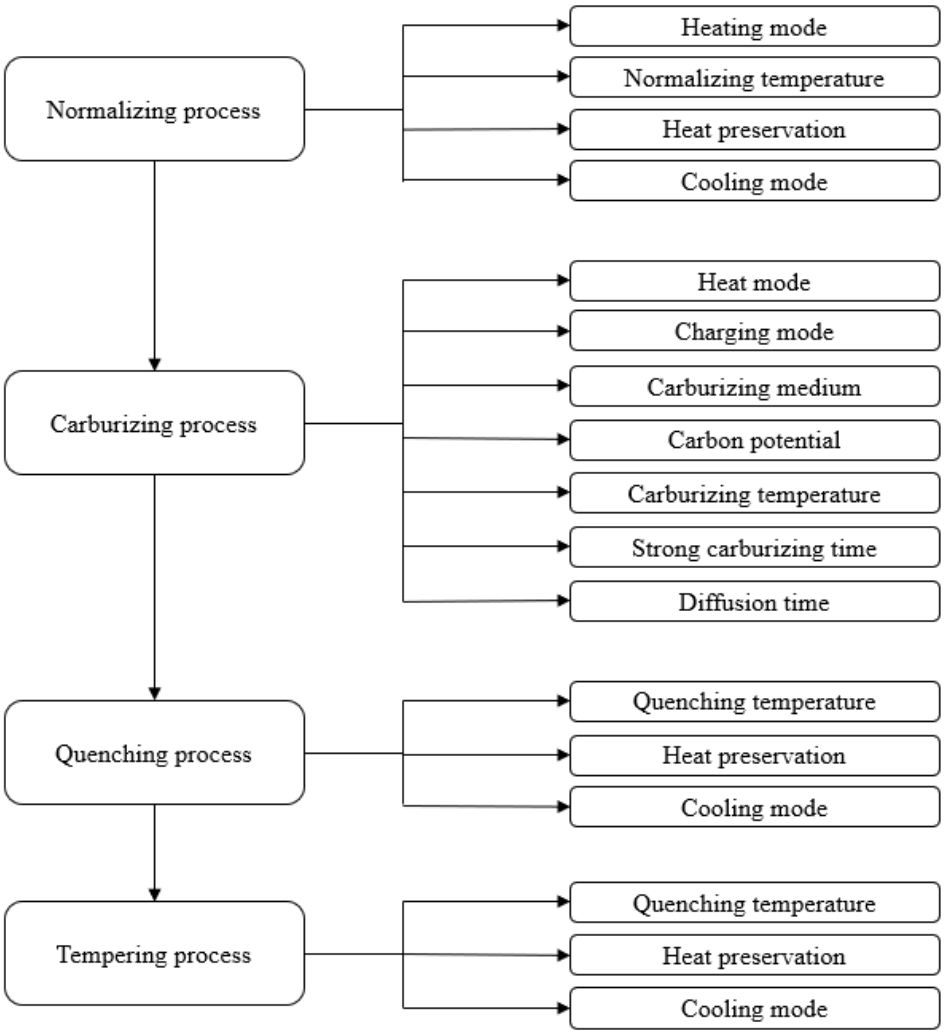

Figure 3-2 Heat treatment: first-level and Second-level processes [30]

From [30], it is noted that manufacturing process parameters are 2.5h time for strong carburizing at 920 ºC temperature, 1.5h time for diffusion at 880 ºC, and fatigue limit is 1644.44 MPa. The Table 3-1shows fatigue life of gears with different toque loads.

Table 3-1Fatigue life of gears with different torque loads [30]

Torque(N*m)	Fatigue life of gears (h)
800	2376.1
900	507.2
1000	310.5
1100	199.1
1200	132.6
1300	91.2

3.2 Axle: Manufacturing and Properties

[31] Axle is a crucial part of automobile that connects wheels on the left side to the wheels on right side, and has a purpose to rotate gear or wheel. The axle is a rigid shaft located at the centre that transmits power from the engine to wheels. Some general machineries of an axle are spider, slip yoke, weld yoke, bearing cup, propeller, and balancing weight that depends on the axle design.

[32] The assembly line of axle manufacturing consists of welding process, plastic injection, straightener, weight balance, assembly, painting, and sequencing. The assemble shop is needed for rear axle that consist of differential and transmits power to wheels. The tag axle or dummy axle does not have much assembly to be done. Figure 3-3 Axle manufacturing processes shows assemble line of axles.

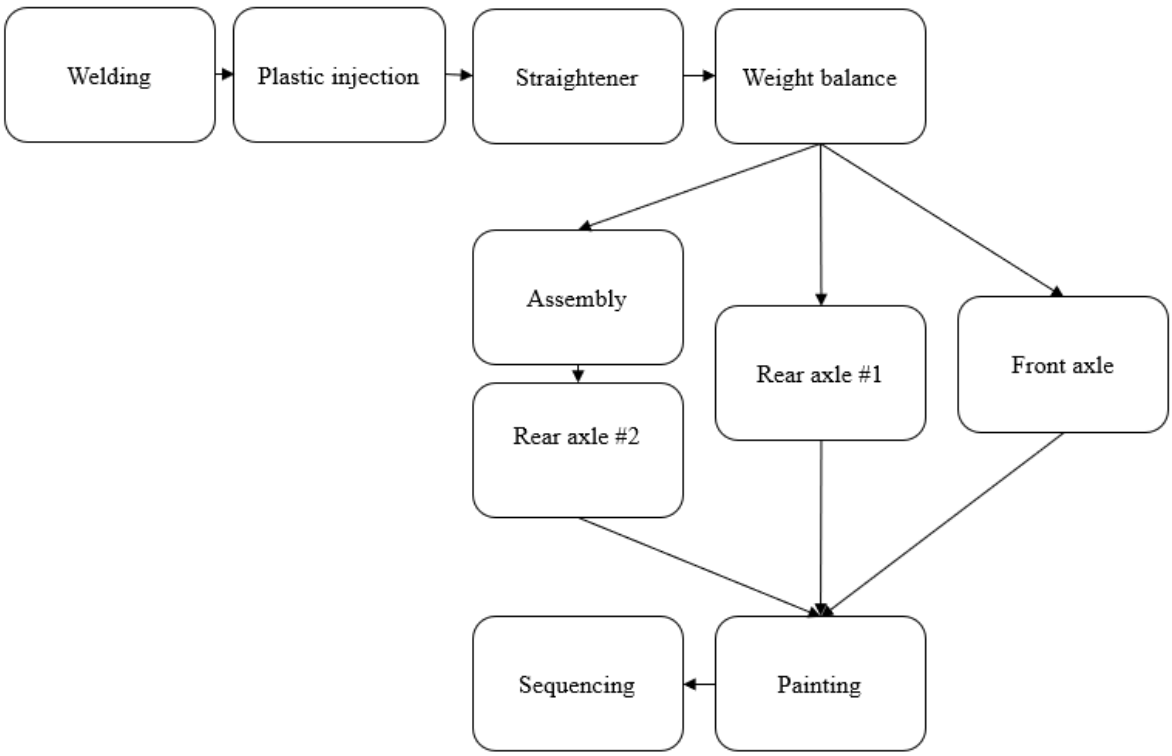

Figure 3-3 Axle manufacturing processes [31]

The axles undergo several heat treatment processes to attain required strength.

I. *Preheating:* To protect axles against distortion and cracking, alloy-steel shafts are preheated in a ternary eutectic chloride mixture at about 600 ºC.
II. *Normalising:* Heated to 845 ºC to 925 ºC and held for minimum 1h time and air cooled.
III. *Annealing:* Heated to 830 ºC to 870 ºC and held for 1h time, and furnace cooled at a rate of around 15 ºC/h to 480 ºC and then air cooled.
IV. *Hardening:* Heated to 830 ºC to 870 ºC and held for 1h time and then oil quenched.
V. *Tempering:* Tempered to 0.5h to 2h time at 175 ºC to 230 ºC and air cooled. To avoid blue brittleness, tempering around 230 ºC to 370 ºC should be avoided.

Drive axles are subjected to heavy torque loads. A 1,300 hp drag race car's drive axle must together bear a torque of 1,356 Nm. With aid of heat treatment processes at above mentioned temperatures, yield strength of 1380 MPa and above can be obtained.

3.3 Shaft: Manufacturing and properties

[33] An automotive drive shaft (also known as propeller shaft) transmits power from the engine to the differential gearbox of a rear wheel drive (RWD) vehicle. The steel drive shaft is generally manufactured in two pieces to so as to increase the fundamental bending natural frequency. Since the bending natural frequency of a shaft is inversely proportional to square of beam length and is proportional to square root of specific modulus. Figure 3-4 Driveline for conventional rear wheel drive (RWD) vehicle shows driveline of a conventional rear wheel drive automobile, including the propeller shaft.

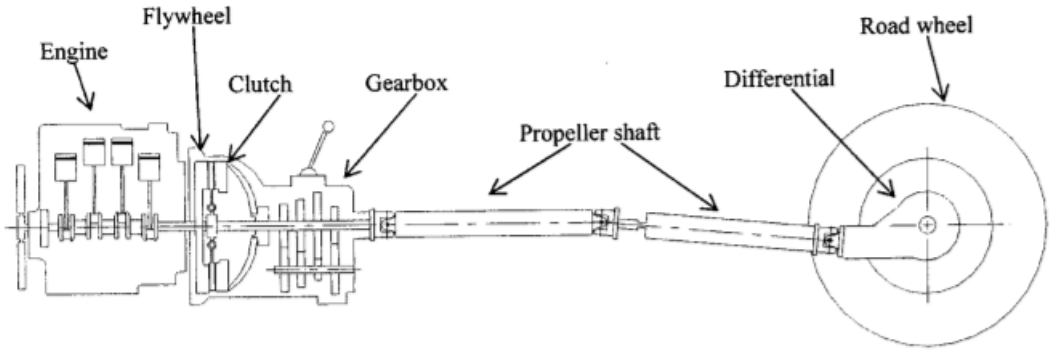

Figure 3-4 Driveline for conventional rear wheel drive (RWD) vehicle [34]

The design of a drive shaft must satisfy three design conditions: static torque capability, buckling torque capability, and bending natural frequency.

The manufacturing process of a hybrid shaft consists of following steps:

I. Stacking up of four carbon fibre epoxy composite layers, and one glass fibre epoxy composite layer on a mandrel.

II. Next, inserting the mandrel with the covered composite layers in the aluminium tube.

III. Stacking up the composite layers, rotating the mandrel with pressure on the inside surface of aluminium tube.

IV. Insert a vacuum bag, and fixing caps that have a vacuum line, and O-rings.

V. Application of pre-load, and curing the vacuum bag by degassing moulding method.

[35] A drive shaft, or propeller shaft should have a torque transmission capability of 3500 Nm or larger, for passenger cars, small trucks, and vans. [36] And the fundamental bending natural frequency should be greater than 9200 rpm to avoid whirling vibrations. Meanwhile the fundamental bending natural frequency of a one-piece drive shafts made up of steels or aluminium is generally lower than 5700 rpm with length of shaft being about 1.5m. An experiment by [33] shows that, a 250mm length specimen (shortened shaft) shaft buckled at a maximum torque of 4320 Nm. Buckled specimen after the static torque test is shown in Figure 3-5 A buckled specimen after the static torque test.

Figure 3-5 A buckled specimen after the static torque test [35]

Another experiment by [35] found that, in fatigue test the hybrid shaft failed after 10^7 cycles under dynamic torque of ±500 Nm.

3.4 Flex Plate: Manufacturing and properties

[37] A flex plate is an automotive part that is installed in automobile engines to deliver torque to transmission. It is manufactured by hot press forming method, by this technique, there is substantial increase of strength through quenching of heated high carbon steel. Advanced dimensional stability after forming through the press operation at high temperatures can be obtained. Figure 3-6 Flex plate manufactured by hot press forming technique.

The material used for the work is commercial steel SK5 with a carbon content of 0.85 wt% from South Korean steel-making company POSCO. The detailed chemical composition of SK5 steel is listed in Table 3-2.

Figure 3-6 Flex plate manufactured by hot press forming technique [37]

Table 3-2 Detailed chemical composition of SK5 steel [37]

C	Si	Mn	P	S	Cr	Ni	Mo	Al	V
0.816	0.176	0.402	0.011	0.001	0.151	0.017	0.001	0.008	0.003

High hardness and good dimensional accuracy of a manufactured flex plate is vital. As it is tough to apply conventional cold forming methods to manufacture the flex plate, hot press forming is introduced with high carbon content steel SK5 as explained in Table 3-2 . The press and die used for manufacturing flex plate are divided into three sections that control the amount of extra stamping.

The brief manufacturing process of flex plate is as follows:

I. The flex plate is 90% pre-formed at room temperature, and then heated up to about 900 ºC to austenize it completely.

II. It is then mounted in a press by a specifically designed transfer unit.

III. In the next process, the flex plate is formed at high temperature with additional punch displacement.

IV. In the final step, it is quenched and cooled with oil.

The main steps of manufacturing process are summarized in Figure 3-7 Flex plate manufacturing process.

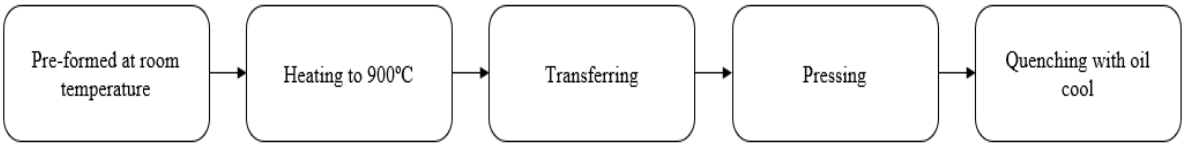

Figure 3-7 Flex plate manufacturing process [37]

To attain proper hardness, proper heat treatment process should be selected. The considered heat treatments are: Austempering and quenching and tempering. The treatments are performed at same austenizing temperature of 870 ºC for a duration of 600s. The heat temperature is varied with 60 ºC intervals for austempering process and 20 ºC for quenching and tempering process to obtain optimal values. After austenizing for about 60 minutes, the specimen is water cooled, whereas air cooling is used for quenching and tempering process.

4 MICROALLOYING OF FORGING STEELS UNDERGOING CONTROLLED COOLING

Metal forging is a process where in metals are formed, shaped by the use of compressive forces. The forces may be delivered using hammering, pressing, or rolling. Based on working temperature of metals, forging process is classified into cold forging, warm forging, and hot forging.

4.1 Types of Forging Steels Undergoing Controlled Cooling

[38] Direct cooling process has become more frequently used substitute for traditional quenching and tempering process for heat treatment of steels. This is because of the fact that direct cooling offers a good combination of strength and ductility at significant cost savings. Hence, it is finding more applications in the field of automobiles. The application of alloy elements and controlled cooling processes depends on a synergic combination of plastic deformation and heat treatment, which is now a common way to reduce costs of manufacturing processes and to improve mechanical properties of a forged parts.

Efforts to introduce Nb into steel for hot-rolled sheets and other processes gave rise to development of an important group of micro-alloyed steels, that are significant for technical and economic reasons. The benefits micro addition of Nb in steels were revealed completely in High Strength Low Alloy (HSLA) steels. The final properties of HSLA steels are achieved directly after deformation process as a result of controlled cooling process. At the present time, direct cooled steel parts can achieve typically bainite, martensite, ferrite-pearlite, or different bainite-martensite structures.

There are several types of steels used for forging process which are discussed below:

I. *38MnSiVS6*: A study by [38] discovered that the final properties of 38MnSiVS6 exhibited a Ultimate Tensile Strength (UTS) of 820 MPa, Tensile Yield Strength (TYS) of 550 MPa, elongation of 12%, and area reduction of fracture 22%. These properties meet the requirements of typical automotive high-pressure pump crankshaft.

II. *38MnSiVS5*: [39] This is a medium carbon micro-alloyed steel. The finished forging temperature, quenching temperature, and post-annealing temperature, and time affect the properties significantly. The chemical composition of this steel is (wt%): Fe-0.38 C-0.68 Si-1.5 Mn-0.022 P-0.06 S-0.18 Cr-0.06 N-0.11 V. Other elements like Ti, Nb, if at all present are below the detection level.

III. *QStE380*: [40] J. Zrnik and team used QStE380, a Ti-Nb micro-alloyed steel to analyse the austenite deformation behaviour during thermomechanical processing. The steel also contained C, Mn, Al, Nb, Ti, Si, S, P, Zr.

IV. *Steel manufactured by Iran Alloy Steel Co.*: [41] A steel containing C, Mn, Si, Nb, Ti etc was supplied to students of materials engineering department, Ferdowsi University of Mashhad (FUM). The goal of study was to conduct new process route for hot forging of Nb containing micro-alloyed steels.

Detailed chemical composition of steels mentioned above has been presented in Table 4-1 Chemical composition of various steels

Table 4-1 Chemical composition of various steels [38] [39] [40] [41]

	Elements, contents in %												
Name of steels	C	Si	Mn	P	S	V	Al	Cr	N	Nb	Cr	Ti	Zr
38MnSiVS6	0.36	0.56	1.35	0.008	0.055	0.08	0.012	-	-	-	-	-	-
38MnSiVS5	0.38	0.68	1.5	0.022	0.06	0.11	-	0.18	0.11	-	-	-	-
QStE380	0.1	0.02	0.91	0.011	0.008	-	0.04	-	-	0.031	-	0.041	0.005
Iran alloy steel co.'s steel	0.24	0.28	1.538	0.011	0.028	0.12	0.026	0.197	0.013	0.049	0.197	0.002	-

4.2 Process Route of Forging Steels

There is also another classification of forging process, other than temperature, that is based on type of forging process. They are classified as open die forging, closed die forging, and roll forging. All these process have different routes but the basic principle of application of forces at various temperatures remains the same.

I. *Open die forging*: In this type of forging, heated metal workpiece are given shape between a top die attached to a ram and a bottom die attached to an anvil or hammer. The metal part in open die forging is never entirely confined or restrained in dies. Characteristically, temperature ranges from about 260 ºC to 1300 ºC, appropriate temperatures are applied while working on metal parts. Once the metals are heated to required temperature, intricate hammering or pressing of the workpiece is performed to progressively to shape metal to its desired form. Typically, larger, simple shaped parts such as bars, rings, or hollows are produced using open die forging process.

II. *Closed die forging*: In closed die forging, the die moves towards each other, thus covering the workpiece completely or partially. There is heated raw material that is almost the shape and size of the final forged part and is placed in the bottom die. This method works by including the shape of the forging into the top or bottom die as a negative image. Once the process is stared, the impression of top die on the raw material forms it into the required shape and size. This process can be used to manufacture parts that range in size from few kilograms to about 25 tons. Gears, connecting rods are some automotive parts manufactured by closed die forging.

III. *Roll forging*: Roll forging, also called as roll forming., is a process of forging that uses opposite rolls to form the metal part. Although, roll forging uses rolls to manufacture parts and components , it is still regarded as a metal forging process, and not as a rolling process. The process route involves two cylindrical or semi-cylindrical horizontal rolls that is used to deform raw material. By this process, the thickness is reduces, and also the length increases. The components produced through roll forging have a superior mechanical properties than those produced from other processes.

The Figure 4-1 Schematic representation of open die forging, closed die forging, roll forging shows schematic representation of open die forging, closed die forging, and roll forging.

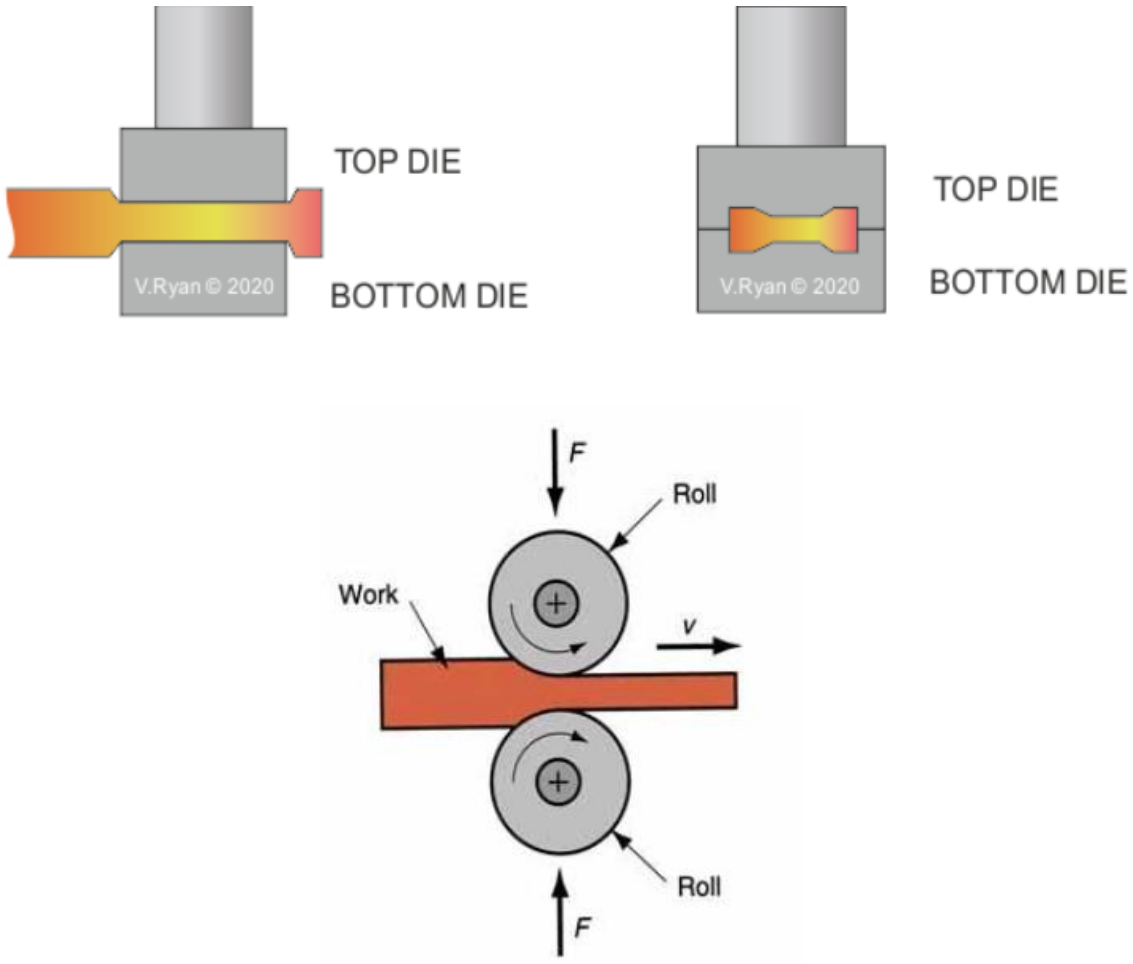

Figure 4-1 Schematic representation of open die forging, closed die forging, roll forging [42]

4.3 Microstructure Evolution due to Addition of Niobium in Forged Parts undergoing Controlled Cooling

In this section, changes/evolution in microstructure of parts that undergo forging process with controlled cooling has been discussed.

CASE STUDY 1: [41] The microstructure study of forging process has been carried out. Figure 4-2 shows microstructure evolution in Niobium micro-alloyed steels undergoing forging and cooling at different rates. The specimen used in the study is a steel billet supplied by Iran Alloy Steel Co. (chemical composition is mentioned in Table 4-1). The billet has a diameter of 65mm and a length of 600mm. The billet was used as raw material for hot-forging process.

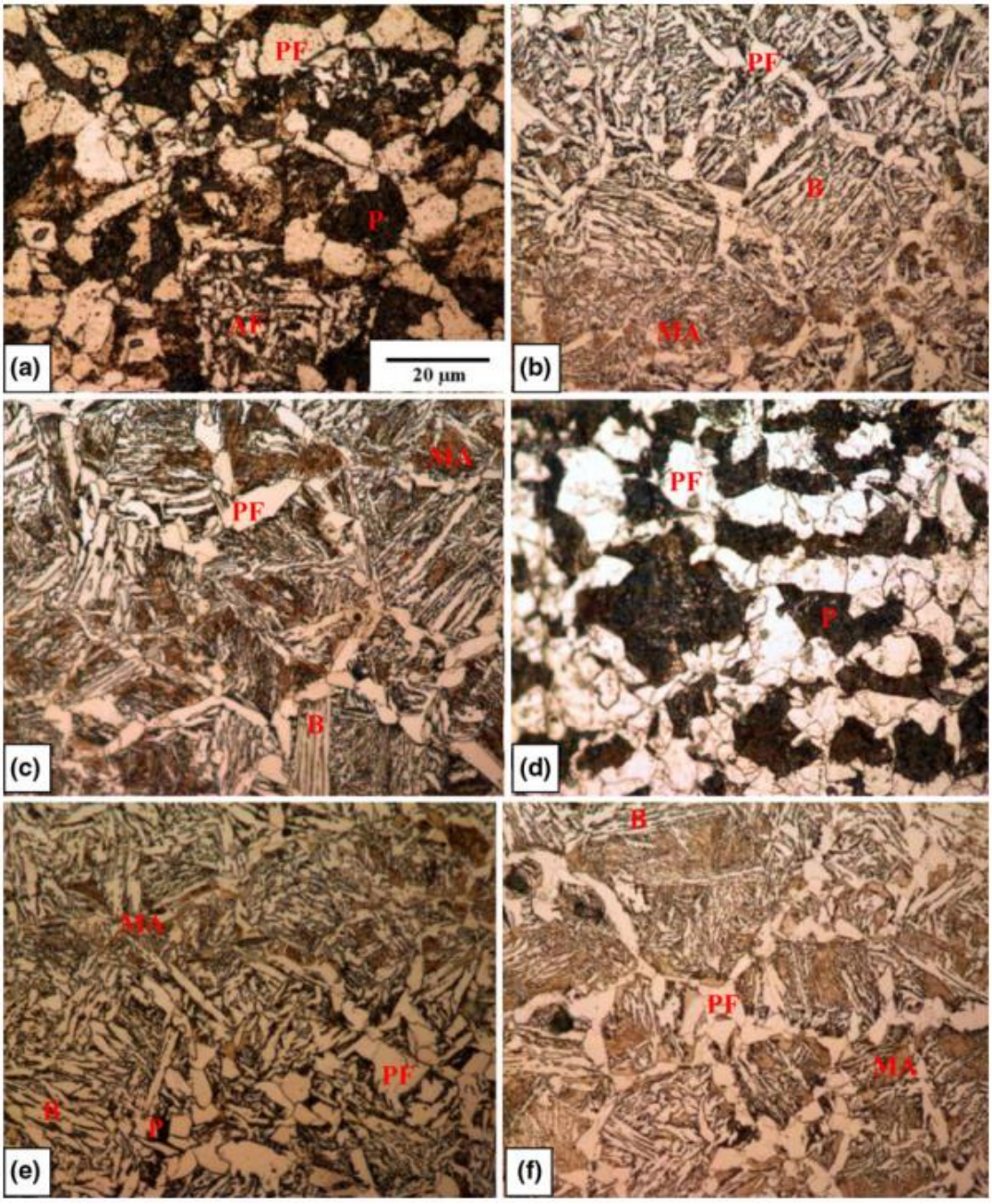

Figure 4-2 Microstructure steel sample forged and a) 30% still air cooled specimen. b) 30% compressed air cooled specimen. c) 30% water spray cooled specimen. d) 50% still air cooled specimen. e) 50% compressed air cooled specimen. f) 50% water spray cooled specimen [41].Abbreviations are mentioned in Table 4-2

Figure 4-2 demonstrates the micrographs of forged specimens with 30% and 50% decrease of height after being cooled with the help of still air, compressed air, and water spray cooling system. In Figure 4-2(a), polygonal ferrite, pearlite and fine packets of ferrite are the main parts of the microstructure for 30% air cooled sample. Although, increasing the cooling rate by the use of compressed air has altered the microstructure of the specimen to polygonal ferrite (at the grain boundaries) and bainite, with a small percentage of mixed phases containing

martensite and retained austenite. In the sample cooled with water spraying system, polygonal ferrite, less percentage of bainite, and more of martensite tend to form. Remarkably, pearlite is substituted by bainite and micro-alloyed constituents at a higher cooling rates. In order to examine the effect of reduction of microstructure evolution, a 50% reduction of height was applied to the specimens, which were later cooled using above mentioned cooling techniques. As it can be seen in Table 4-2 and Figure 4-2(d), for still air cooling, polygonal ferrite and pearlite appear to be principal constituents of the microstructure. Concerning the 50% compressed air cooled specimen in forged condition, polygonal ferrite (on former to austenite grain boundaries), pearlite, bainite and acicular structure can be observed in Figure 4-2(e). In Figure 4-2(f), water spray cooling with highest cooling rate has altered the microstructure to bainite, polygonal ferrite, and martensite.

Overall, a modest banding was seen in most of the samples that were observed. Furthermore, an increase in cooling rate promotes the formation of micro-alloyed structures. The microstructure of specimen with 50% height reduction was found to be desirable because of the fact that the quantity of acicular ferrite was negligible. The compressed air cooling has resulted in more favourable microstructure, that consists of less pearlite and micro-alloyed phases, and more polygonal ferrite, particularly on prior to austenite grain boundaries with a reduced fraction of acicular ferrite (refer Figure 4-2(f)).

Table 4-2 Microstructure of examined specimen in as-forged condition [41]

Condition	Microstructure
30% still air cooled	36% polygonal ferrite (PF), 52% pearlite (P), 12% fine packets of acicular ferrite (AF).
30% compressed air cooled	21% polygonal ferrite (on grain boundaries), bainite (B) and micro-alloy (MA).
30% water spray cooled	20% polygonal ferrite, small fraction of bainite, and more of micro-alloy.
50% still air cooled	49% polygonal ferrite, 51% pearlite.
50% compressed air cooled	18% polygonal ferrite, 8% pearlite, bainite, and micro-alloy.
50% water spray cooled	25% polygonal ferrite, bainite, and significant amount of micro-alloy.

CASE STUDY 2: [43] The effect of cooling rate on the microstructure, mechanical properties of Nb micro-alloyed steels which were treated as structural beams at three various cooling rates has been discussed. The composition of steel in terms of percentage (%) is as follows: C 0.030-

0.100, Mn 0.500-1.500, V 0.001, Nb 0.020-0.050, Si 0.15-0.25, P 0.010-0.020, S 0.015-0.025, N 0.009-0.010.

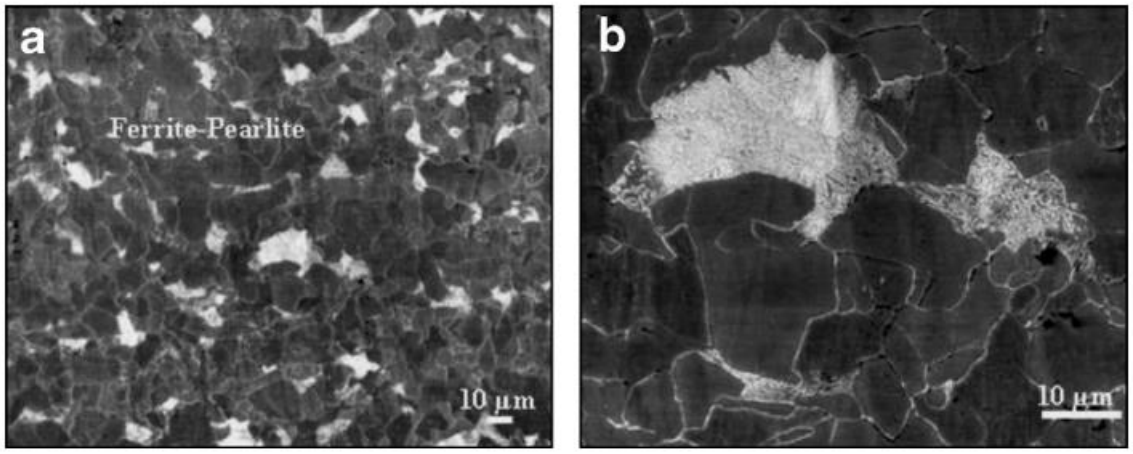

Figure 4-3 Representation of low and high magnification scanning electron micrographs of Nb-micro-alloyed steel processed at (a and b) low cooling rate [43]

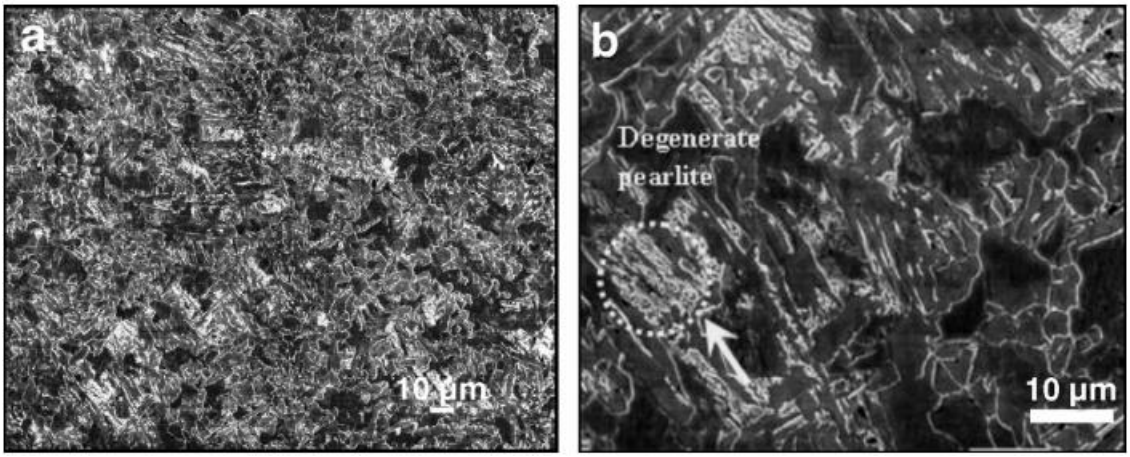

Figure 4-4Representation of low and high magnification scanning electron micrographs of Nb-micro-alloyed steel processed at (a and b) intermediate cooling rate. The figure (b) shows degenerated pearlite [43]

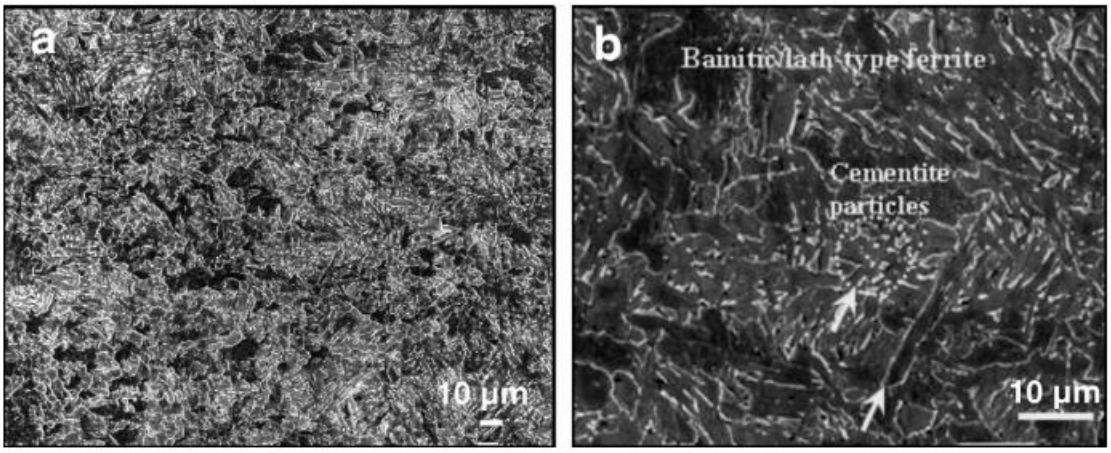

Figure 4-5. Representation of low and high magnification scanning electron micrographs of Nb-micro-alloyed steel processed at (a and b) high cooling rate. [43]

Representation of low and high magnification scanning electron micrographs of Nb micro-alloyed steels that were processed at various cooling rates have been shown in Figure 4-3, Figure 4-4, and Figure 4-5. The principal microstructures elements at low cooling rates were polygonal ferrite and pearlite. At intermediate cooling rates and high cooling rates , the microstructure comprised of lath type/ bainitic ferrite, and degenerated pearlite along with conventional ferrite-pearlite. With an increase in cooling rate, an increased tendency towards formation of lath ferrite/ bainitic ferrite with consequential decrease in conventional ferrite-pearlite microstructure. The microstructure transformation from low to intermediate to high cooling rate may be summarized as ferrite-pearlite to ferrite-degenerated pearlite to bainitic ferrite. The typical grain size of the steels processed at various cooling rates was similar and in the range of 10-12 µm. The quantitative metallographic data for Nb micro-alloyed steels has been summarized in Table 4-3.

Table 4-3 Microstructural characteristics of Nb micro-alloyed steels [43]

Properties of Nb micro-alloyed steels	Low cooling rate	Intermediate cooling rate	High cooling rate
Microstructure	Polygonal ferrite (PF), lamellar pearlite (LP)	Polygonal ferrite (PF), lamellar pearlite (LP), lath-type/bainitic ferrite (LF/BF), degenerated pearlite (DP)	Polygonal ferrite (PF), Lamellar pearlite (LP), lath-type/bainitic ferrite (LF/BF), degenerated pearlite (DP)
Average grain size (mean intercept length μm)	12 ± 2	11 ± 2	10 ± 1
Ferrite hardness, H_K Area fraction (%)	PF: 155 ± 11 85	PF: 293 ± 20 LF/BF: 350 ± 34 PF: 38 LF/BF: 51	PF: 277 ± 21 LF/BF: 355 ± 22 PF: 19 LF/BF: 79
Pearlite hardness, H_K Area fraction (%)	369 ± 35 15	325 ± 20 DP: 11	366 ± 36 DP: 2

4.4 Effect of Micro-alloying Elements on the Microstructure Evolution

[43] In the previous section, we discussed about the microstructure evolution of forged Nb alloyed steels undergoing controlled cooling at different cooling rates. Here, we will discuss about the effects of micro-alloyed elements on microstructure evolution.

I. At traditional or low cooling rates, the microstructure of Nb micro-alloyed steel mainly constituted of polygonal ferrite-pearlite. At intermediate cooling rate, the microstructure contained degenerated pearlite and lath-type/bainitic ferrite along with traditional ferrite-pearlite. Although, at higher cooling rates the microstructure was largely lath-type/bainitic ferrite.

II. Direct cooling has become a frequently used substitute for traditional quenching-tempering method of treatment of steel products, presenting a good blend of strength and ductility at significant costs savings. Therefore, finding growing number of applications in automotive applications.

III. Additions of micro-alloying elements and controlled processing dependent on a synergic combination of plastic deformation and heat treatment is now a general way of reducing manufacturing costs to improve mechanical properties of a forged parts.

IV. The change in microstructure from largely ferrite-pearlite to predominantly bainitic-ferrite with an increase in cooling rate is accountable for the high strength-toughness mixture of Nb micro-alloyed steels at high cooling rates.

4.5 Mechanical Properties of Forged Niobium Micro-Alloyed Steels Undergoing Controlled Cooling

Some mechanical properties of Niobium micro-alloyed steels undergoing controlled cooling has already been mentioned in Table 4-3. In Table 4-4, some mechanical properties of Nb micro-alloyed steels undergoing cooling at low, intermediate, and high cooling rate has been tabulated. From Table 4-4 it may be noted that as the cooling rate increases, the mechanical properties of the steel enhance. The yield strength and tensile strength both increase from low cooling rate to high cooling rate. Although, the percentage of elongation was nearly similar for different cooling rates.

Table 4-4 Representation of room temperature tensile and impact properties of Nb micro-alloyed steels [43]

Properties of Nb micro-alloyed steel	Low cooling rate	Intermediate cooling rate	High cooling rate
Yield strength (MPa)	420	455	482
Tensile strength (MPa)	503	551	572
% Elongation	26	26	23
Impact energy (Nm) Temperature (F)			
70	222	199	224
40	213	187	221
20	142	172	168
0	152	157	161
-20	68	89	146

5 MICRO-ALLOYING OF FORGING STEELS UNDERGOING QUENCHING AND TEMPERING

In previous chapter, we discussed about Niobium micro-alloyed forging steels undergoing controlled cooling. Here, we will discuss similar Niobium micro-alloyed steels undergoing quenching and tempering processes.

5.1 Types of Forging Steels Undergoing Quenching and Tempering

[44] This chapter emphasise on understanding the effect of Niobium content on phase transformation behaviour and mechanical properties of forged low carbon steel undergoing direct quenching. The investigated steels had three various levels of Niobium: 0 wt%, 0.02 wt%, and 0.05 wt%.The purpose of the study is to discover the possibilities for optimizing the strength, toughness balance of a potentially low carbon steel, that is acknowledged to deliver a good basis for tough, direct quenched martensite structure. [45] In the event of direct quenching, enhanced strength composed with low temperature toughness can be attained by straining the austenite, in the no-recrystallization regime lower the recrystallization stop temperature (RST) prior to quenching process. This way, the hardness of altered martensite surpasses the hardness achievable in the steel with the same carbon content after applying simple reheating and quenching.

[46] Addition of Niobium in steels in small quantities is known to be beneficial in attaining a finer grain structure because of its ability to control the austenite grain size during reheating of slab by pinning effect of NbC precipitates and also, refining grain size during subsequent deformation and recrystallization in the hot rolling stage. [47] It has been noted that Niobium can improve hardenability in solid solution, but the formation of niobium-carbides, if any, can be counterproductive thus reducing the hardenability. Nevertheless, it is not completely understood the effectiveness of Niobium in steels at the yield strength of 1000 MPa or higher. Some examples of Niobium micro-alloyed forged steels that undergo quenching and tempering are discussed below:

I. *49MnVS3*: [48] For closed die forgings in automobile industry, a steel grade with Si, Mn, S, V was established in the mid-1970s. Although, the required strength

could be attained by 0.08% Nb micro-alloying when high processing temperatures are applied, limited toughness restricted the applications. For improved toughness another steel with 0.03% Nb was developed suitable for forging of automobile parts like connecting rods etc.

II. *16Mn5Cr*: [49] Steels like 16MnCr5 and 20MnCr5 can show excess grain growth when they are heated above 960 ºC. These steels when micro-alloyed with Nb can raise grain coarsening temperature significantly with an increase in Nb.

The table shows chemical composition of various forged steels with their base composition as well as micro-alloyed composition.

Table 5-1 Chemical composition of forged steels undergoing quenching and tempering [48] [49]

Names of steel	C	Si	Mn	P	S	Cr	Mo	Ti	Nb	Al	B	N	V
49MnVS 3	0.50	0.25	0.70	-	0.040	-	-	-	-	-	-	-	0.10
16Mn5Cr - Base	0.18	0.22	1.05	-	-	0.92	-	-	-	0.033	-	0.008	-
16Mn5Cr + Nb	0.22	0.22	1.20	-	-	1.01	-	-	0.024	0.026	-	0.013	-
16Mn5Cr + NbTi1	0.17	0.28	1.14	-	-	1.19	-	0.007	0.030	0.029	-	0.026	-
16Mn5Cr + NbTi2	0.17	0.30	1.35	-	-	1.12	-	-	0.055	0.016	-	0.019	-

5.2 Process Route of Forged Steels undergoing Quenching and Tempering

[49] One of the initial developments of micro-alloying in long products was low carbon micro-alloyed steel wire rods for applications of cold heading (example bolts). In traditional cold heading steels, a spherodizing process is done to soften the medium carbon steel with the aim to carry out cold forming operations like wire drawing and cold heading, and further, a quenching and tempering treatment is done so as to obtain desired mechanical properties.

It is, although, possible to entirely remove the wire annealing and quenching and tempering treatments while manufacturing of cold headed bolts or similar products by the use of low carbon steel micro-alloyed with niobium. Therefore, with the removal of intermediate heat treatments from the manufacturing process, there is significant savings in manufacturing costs.

Also, there is less carbon emission due to eliminated processes that makes manufacturing environment friendly. Figure 5-1 shows processing steps of conventional steels and micro-alloyed steels.

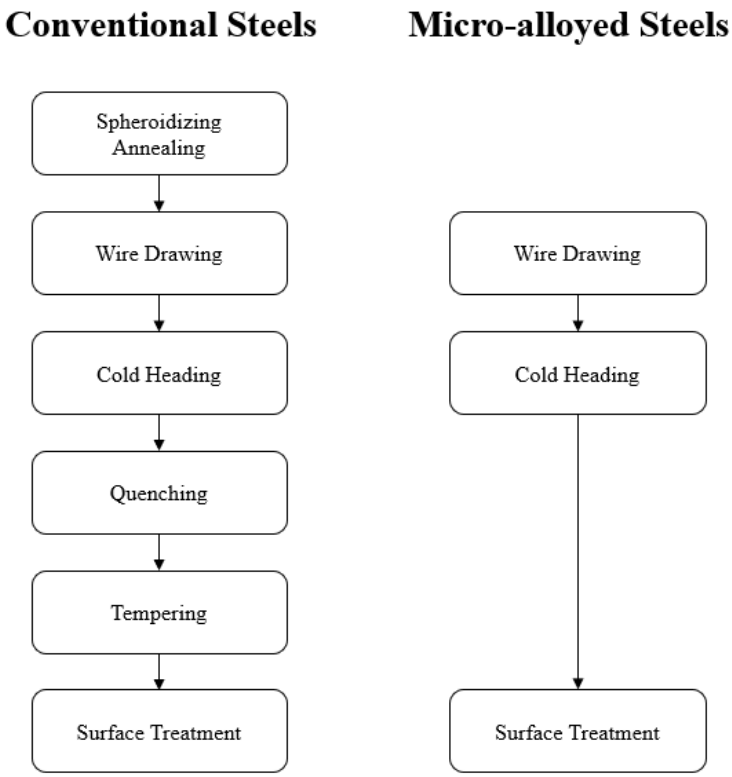

Figure 5-1 Comparison of processing steps for manufacturing of conventional steels and micro-alloyed steels [49]

[48] According to a study by [48], with the adoption of niobium micro-alloyed steels to manufacture non-heat treated bolts, it is possible to completely eliminate quenching and tempering process. This will result in enormous cost savings. The new process route is shown in Figure 5-2.

Figure 5-2Processing steps for manufacturing of non-heat treated bolts using Nb micro-alloyed steels [48]

5.3 Microstructure Evolution due to Addition of Niobium in Forged Parts undergoing Quenching and Tempering

[44] Figure 5-3 represents characteristic microstructures of steel at a depth of one-fourth of the samples for both the finish rolling temperatures (FRTs). The microstructure comprised of fine packets and blocks of martensitic laths oriented in different directions. Auto-tempering of martensite leading to the precipitation of fine carbides in martensite laths was likewise evident in some sections as shown in Figure 5-3 with red arrows. Based on microstructure characterisation, both the FRTs formed mainly martensitic microstructures in all cases.

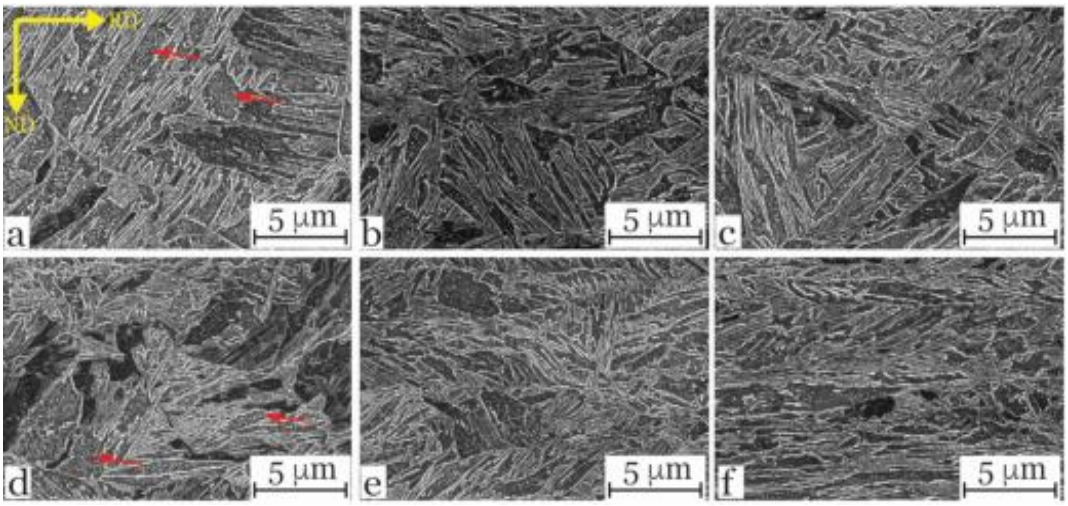

Figure 5-3 Microstructures of steels; upper row: FRT 920ºC, lower row: FRT 820ºC. (a,d) DQ, (b,e) DQ+0.02Nb, (c,f) DQ+0.05Nb [44]

The elongated martensitic structure may be realised particularly in the case of 0.05Nb steel prior to being strained with low FRT (refer Figure 5-3f).

Figure 5-4 shows an example of a lath martensite structure that was examined by transmission electron microscopy (TEM) of DQ+0.02Nb steel with 820ºC FRT. The martensite lath structure may be realised with a characteristic lath width of 50-100 nm combined with high density of dislocation networks throughout the sample. A comparable microstructure was seen in various other investigated steels with practically no significant differences.

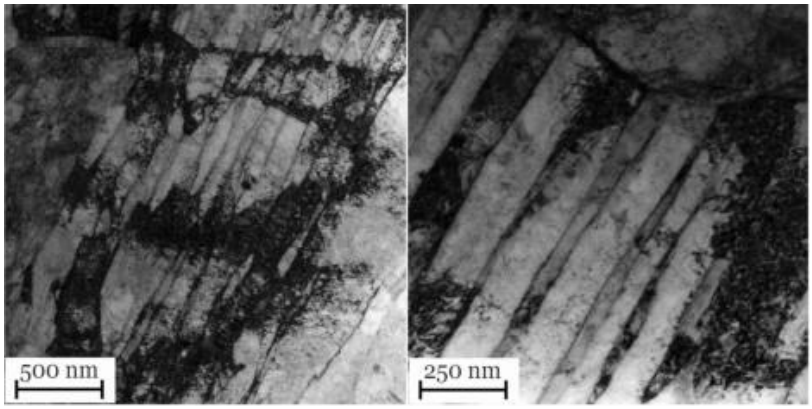

Figure 5-4 Transmission electron microscopy (TEM) microstructures of DQ+0.02Nb steel with FRT 820ºC [44]

[44] Effective grain (> 15º) and lath size (2.5º-15º), calculated as equivalent circle diameters (ECD) were presented. Lesser FRTs and higher quantity of niobium produced very smaller mean grain sizes owing to higher degree of austenite packing.

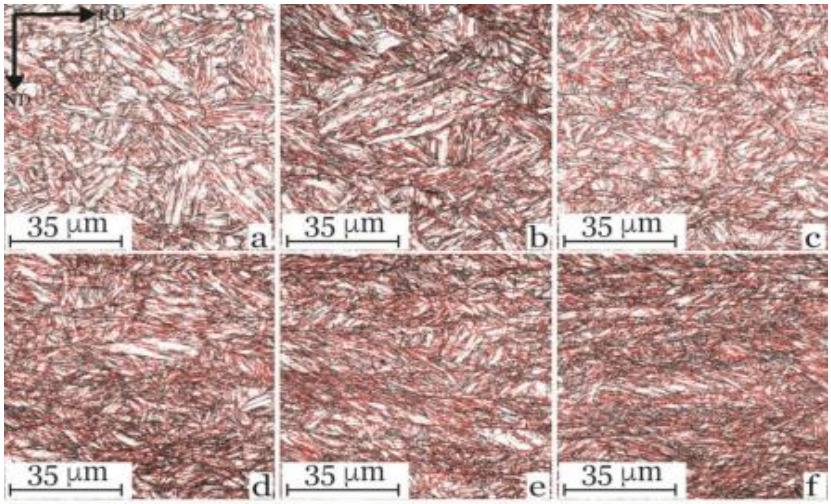

Figure 5-5 Low angle (2.5º-15º, red lines) and high angle(>15º, black lines) boundaries of steels. Upper row: FRT 920ºC, lower row: FRT 820ºC. (a,d) DQ, (b,e) DQ+0.02Nb, (c,f) DQ+0.05Nb. [44]

From effective grain sizes at 90% in the cumulative size distribution , it is clear that 90th percentile effective high angle grain size changes significantly more than the mean values and that its behaviour as a function of niobium content depends on the FRT. Figure 5-5 Low angle (2.5º-15º, red lines) and high angle(>15º, black lines) boundaries of steels. Upper row: FRT 920ºC, lower row: FRT 820ºC. (a,d) DQ, (b,e) DQ+0.02Nb, (c,f) DQ+0.05Nb. depicts the low and high angle boundaries of the steels that were studied based on the Electron backscatter diffraction (EBSD) analysis. Higher quantity of low angle boundaries (red lines) was achieved with the low FRT and higher niobium content. The development of densely pancaked austenite

structure increased the number of low angle boundaries of the martensitic structure, that is observed clearly in Figure 5-5f.

5.4 Effect of Micro-alloying Elements on the Microstructure Evolution

[44] The effect of niobium on the microstructures and mechanical properties of hot rolled and direct quenched 6mm thick steel having 0.08 wt% C has been studied. Finish rolling temperatures (FRT) of 820ºC and 920ºC were used to attain various levels of pancake structures in austenite and the rolled plates were directly quenched to room temperature at a rate of 90 ºC/s. Based on the results, the below mentioned conclusions were drawn for the compositions and conditions:

I. [44] The microstructures of directly quenched specimens consisted of lath martensite and few lower bainite. Smaller lath and effective grain sizes were accomplished with higher niobium content and the lower finish rolling temperature of 820 ºC. Niobium alloying also increased the quantity of low angle boundaries in the microstructure.

II. [44] Niobium micro-alloying leads to improved strengths in steels. The highest effect on niobium on strength was seen at the higher finish rolling temperature of 920 ºC, where the effect of niobium on austenite pancaking was the strongest. When low finish rolling temperature of 820ºC was used, high strengths were attained even in the case of niobium free steel and the effect of niobium was smaller.

Addition of 0.02wt% of niobium together with low finish rolling temperature produced the overall best mechanical properties and may be considered to be in high level compared to steels with similar strength.

III. [49] The important effect of niobium in engineering steels are of three types: Firstly, the grain refinement of austenite at high temperature during reheating before hot rolling/heat treatment.

Secondly, lowering of austenite to ferrite transformation temperature. And thirdly, precipitation of fine niobium carbonitride particles that strengthen ferrite.

IV. [49] The grain refinement effect of niobium on austenite is the most extensively used effect of niobium in the heat treatment of engineering steels

5.5 Mechanical Properties of Forged Niobium Micro-alloyed Steels Undergoing Quenching and Tempering

[44] The results of tensile test of the investigated steels are tabulated in Table 5-2. The FRT of 820ºC formed yield strength of over 1000MPa in all cases and the values for niobium micro-alloyed steels are higher than base steel without niobium. The lower FRT developed highly elongated austenite. In contrast, the biggest effect of niobium on strength was revealed at FRT of 920ºC where the effect of niobium on austenite pancaking was the strongest. A high degree of deformation in austenite was attained by niobium alloying at higher FRT, that resulted in a visible increase in yield strength and tensile strength. Adding more than 0.02% niobium did not provide much increase in yield strength, but there was small improvement in the tensile strength. Generally, the advantage of niobium micro-alloy on strengthening is achieved by the use of high FRTs.

Table 5-2 Tensile properties, Charpy V impact properties of forged steels ;Agt is the total uniform elongation (elastic +plastic) as defined in ISO 6892-1:2009 [44]

Finish rolling temperature (FRT)20	Steel type	Yield strength (MPa)	Tensile strength (MPa)	Elongation (%)	Agt (%)	Transition temperature (°C)	Upper shelf temperature Tus (°C)	Upper shelf Energy Eus (°C)
920 °C	DQ	943 ± 20	1151 ± 11	12.2 ± 0.3	3.1 ± 0.1	-66	50	130
	DQ+ 0.02Nb	1014 ± 6	1195 ± 8	11.2 ± 0.4	3.1 ± 0.0	-56	50	121
	DQ+ 0.05Nb	1011 ± 14	1208 ± 10	12.2 ± 0.7	3.0 ± 0.1	-53	50	112
820 °C	DQ	1022 ± 3	1215 ± 1	12.2 ± 0.6	2.8 ± 0.1	-67	20	107
	DQ+ 0.02Nb	1067 ± 8	1245 ± 8	12.2 ± 0.2	2.7 ± 0.1	-67	20	112
	DQ+ 0.05Nb	1060 ± 10	1262 ± 6	12.2 ± 1.1	3.1 ± 0.1	-58	20	103

Table 5-2 also gives a summary of important values of Charpy V impact test. Marginally better results of impact toughness properties were seen with FRT of 820ºC in comparison to 920ºC. Bearing in mind the investigated steels and various levels of niobium, the transition temperatures are very close to each other for a given FRT. A marginal deterioration in impact toughness properties may be seen at higher niobium content of 0.05%, presumably as a result of increased tendency of micro segregation.

Generally , it can be concluded that the lower FRT of 820ºCimparted better overall properties, particularly when optimized with 0.02% niobium.

6 MICRO-ALLOYING FOR HIGH TEMPERATURE CARBURIZING

[50] Automotive parts such as transmission system, gears have to satisfy complex requirements. The surface of parts that are forged are often carburized and quenched to make hard surface to a tough core along with exceptional wear resistance and fatigue strength. General carburizing temperatures are about 930ºC to 950ºC. Depending on the depth of carburizing, the time needed for processing can take up to 20 hours or more. Since several years the possibility to reduce necessary carburizing time by increasing the working temperature has been in discussion. [51] By increasing the carburizing temperature, up to 60% of time may be saved depending on the case depth. Although, at these elevated temperatures, there will be considerable austenite grain growth. Micro-alloying steels with niobium may not only avoid grain growth but also generate a more homogeneous fine austenite grain structure. Along with hardenability and chemical composition, the austenite grain size is a very important feature for case hardening steels.

[52] Engine, powertrain and axles account for about 50% of the total cost of a vehicle. Many of these components are produced from special steel grades undergoing casting and forming (forging) operations. Those components that are exposed to contact loads like gears and shafts often need additional heat treatment and surface hardening process to attain an appropriate combination of strength, toughness, and wear resistance.

6.1 Types of Steels Undergoing High Temperature Carburizing

[53] [54] As shown in a study, unique opportunities exists to design enhanced gear steels for high temperature carburizing through the use of niobium additions combined with carefully selected controlled rolling practice. The use of micro-alloys additions for grain size control has become a common practice in the manufacturing of a variety of steels. There are various types of steels used in carburizing process, some of them are mentioned below:

I. *16MnCrS5+NbTi*: [55] The standard DIN 16MnCrS5 was renamed as "16MnCrS5+NbTi" after niobium and titanium were micro-alloyed with steel. The

main changes amongst the chemical composition are the addition of titanium and niobium and higher content of nitrogen of micro-alloyed steel.

II. *16MnCr5+N,Ti,Nb*: [50] Earlier, steels have been alloyed with aluminum and nitrogen to attain sufficient grain stability. In recent times, several results regarding addition of niobium and titanium as a micro-alloy have been published. It has been proven that, a sufficient austenite grain size control during case hardening at temperatures of over 1000ºC can be realized by applying niobium and titanium as well as an aligned ratio of nitrogen and aluminum.

III. *Ti-modified SAE 8620*: [56] Three niobium micro-alloyed steels were modified to a base Ti-modified SAE 8620 steel, were produced as laboratory heats with compositions shown in Table 6-1. These modified steels contained nominally constant levels of carbon, titanium, and nitrogen with various levels of niobium (0.02, 0.06, and 0.1 wt %).

IV. *18CrNiMo7-6*: [57] This type of steels are generally used for medium and large sized gears in Western Europe region. This is a EN 10084 (1.6587) standard steel with a carbon (C) range of 0.15-0.21 wt. %, Mn 0.50-0.90 wt.%, Cr 1/.50-1.80 wt.%, Mo 0.25-0.35 wt.%, and Ni 1.40-1.70 wt. %. The detailed composition is given in Table 6-1.

Table 6-1Chemical composition of metals undergoing high temperature carburizing [56] [50] [55] [57] [58]

Name of steels	C	Mn	P	S	Si	Cr	Ni	Mo	Cu	Al	Nb	O	N	Ti
Ti-modified SAE 8620	0.22	0.85	0.019	0.003	0.25	0.59	0.43	0.20	0.01	0.024	0.1	24*	87*	0.032
16MnCr5+N,Ti, Nb	0.17	1.35	-	-	0.30	1.12	-	-	-	0.016	0.016	-	0.019	0.055
16MnCrS5+Nb Ti	0.18	1.19	0.015	0.022	-	1.05	0.16	0.05	0.16	210*	>300*	-	>100*	>300*
18CrNiMo7-6	0.21	00.90	0.025	0.035	0.40	1.80	1.70	0.35	-	-	-	-	-	-
16MnCr5+Nb	0.19	0.74	0.011	0.012	0.23	1.19	-	-	-	0.041	0.045	-	0.026	0.001

*the compositions are mentioned in ppm.

6.2 Process Routes of steels Undergoing High Temperature Carburizing

[50] Increasing cost pressure on the production of carburized components needs decreasing delivery times. In the field of mechanical processing, heat treatment offers a great potential for cost reductions. By the commencement of direct hardening process, significant savings may be achieved in the field of heat treatment. Additional improvements may be attained by the use of higher carburizing temperatures. The high temperature carburizing offers an enhanced carbon transfer from atmosphere to the components to be manufactured, as well as accelerate carbon diffusion within the components. The comparison between a conventional carburizing process at 930°C and high temperature carburizing process at about 1030°C shows an overall time reduction of about 40% may be achieved (shown in Table 6-2).

Table 6-2 Comparison of required time for several process periods [50]

Vacuum carburization Case depth: 1.5mm (16MnCr5+MAE)		**Temperature 930°C**	**Temperature 980°C**	**Temperature 1030°C**
Loading	h	0.25	0.25	0.25
Heating	h	1.5	1.75	2
Carburization and diffusion	h	8.5	5	3
Cooling to quenching temperature	h	0.75	1	1.25
Quenching and loading	h	0.5	0.5	0.5
Overall	h	11.5	8.5	7
Reduction of time	**h**	**Reference**	**3**	**4.5**
	%		**~25**	**~40**

The cost for hard machining is directly related with the amount of distortion after carburizing. An increasing carburizing temperature does not worsen when quenching is carried out from standard hardening temperature. [59] However, more homogeneous grain size distribution is attained by grain boundary pinning precipitates that will result in a substantial reduction in scatter of distortion. Cost expensive operations like grinding and honing may be reduced or completely avoided. When shared with new process technologies like vacuum carburization with high pressure gas quenching, a substantial reduction of costs within the complete

manufacturing process may be realised. [60] Besides the increased strength and toughness, a fine and homogeneous microstructure offers an improved fatigue behaviour.

However, it is not predictable in what way the different process steps during manufacturing, like, additional annealing, various degrees of deformation, temperatures and deformation rates, affect the appearance of the precipitates that are responsible for the grain size control. An improved process route for high temperature carburizing has been suggested in Figure 6-1

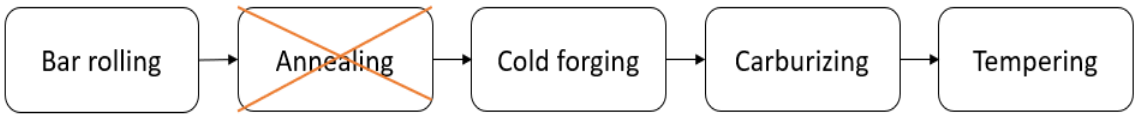

Figure 6-1 New process route for high temperature carburizing [50]

[52] Carburizing steels are used in automotive industry to manufacture case hardened components for engine and powertrain applications.

6.3 Microstructure Evolution due to Addition of Niobium in Steels Undergoing High Temperature Carburizing

[50] [61] The grain coarsening temperature (GCT) is an indicator for microstructure stability and depends on the case of high temperature carburizing, amount of micro-alloying elements and on the precipitates available. The micro-alloying concept of the steel that is investigated is based on a relatively high content of 400ppm of aluminium and 450ppm of niobium. Titanium, which is well known to element to form stable precipitate at high temperature is present only as a tramp element. This steel grade has shown austenite grain stability at up to 1050°C in the as rolled condition.

The behaviour of precipitation was analysed by means of transmission electron microscopy (TEM) using carbon replicas. Due to enlarged quantity of niobium, the 16MnCr5 steel grade has a significant amount of niobium carbides and nitrides, as well as some titanium nitrides.

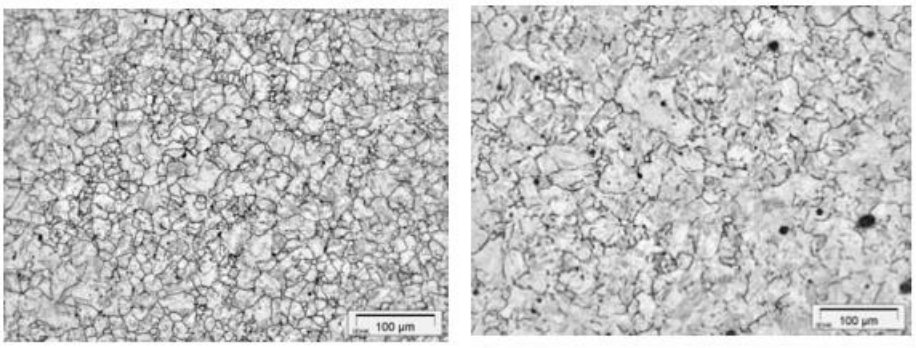

Figure 6-2 Former austenite grain size, after blank hardening of 16MnCr5+Nb steel [50]

Moreover, aluminium nitrides that start to dissolve at temperatures of above 1000°C, these precipitates act as grain boundary pinning particles. This provides an improved grain size stability at higher temperatures that has been established by grain growth investigations. In the case of as rolled condition at temperatures above 1100°C, even the Nb(C,N) and Ti(C,N) coarsen in such a way that grain growth can take place. In Figure 6-2, a comparison between the austenite microstructure and the precipitates state after blank hardening, has been shown. It discloses that with increasing hardening temperature, coarsening of grain boundary pinning particles takes place. The coarse particles grow at the expense of small precipitates. Furthermore, dissolution begins due to the increased solubility at higher temperature.

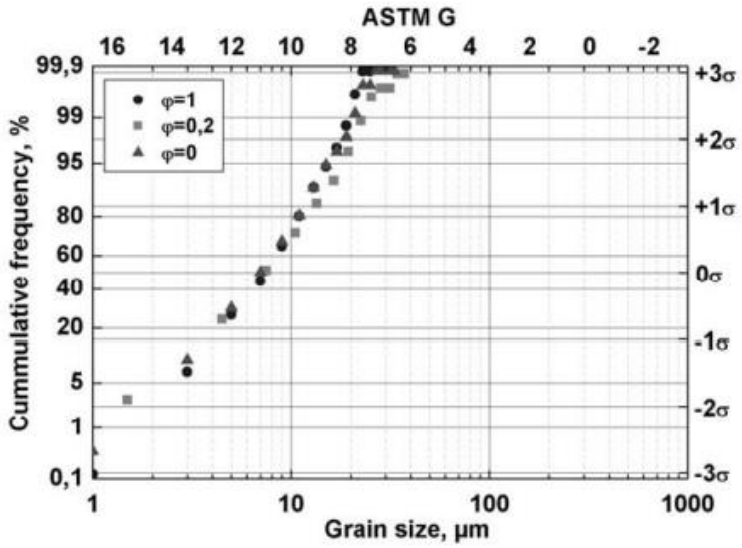

Figure 6-3 Grain size distribution of 16MnCr5+Nb steel after forging at 700°C and blank hardening at 1050°C [50]

Figure 6-3 impeccably illustrates the result of grain growth investigations of 16MnCr5+Nb steel after deformation at 700°C and blank hardening at 1050°C. All the studied conditions (as rolled, $\phi = 0,2;1$) offer a practically identical homogeneous grain size distribution with a mean grain size of ASTM 11. This effect suggests that case hardening can be realised up to temperatures of 1050°C without grain coarsening after forging at 700°C.

A comparable result is attained for deformation temperatures of 900°C (in Figure 6-4) and 1250°C (in Figure 6-5). Due to the substantial amount of micro-alloying elements, niobium containing 16MnCr5 offers good grain size stability. The chosen alloying concept containing aluminium and niobium with traces of titanium, may be carried out without any risk to the current manufacturing process of engineering parts that are designated for high temperature carburizing of up to 1050°C.

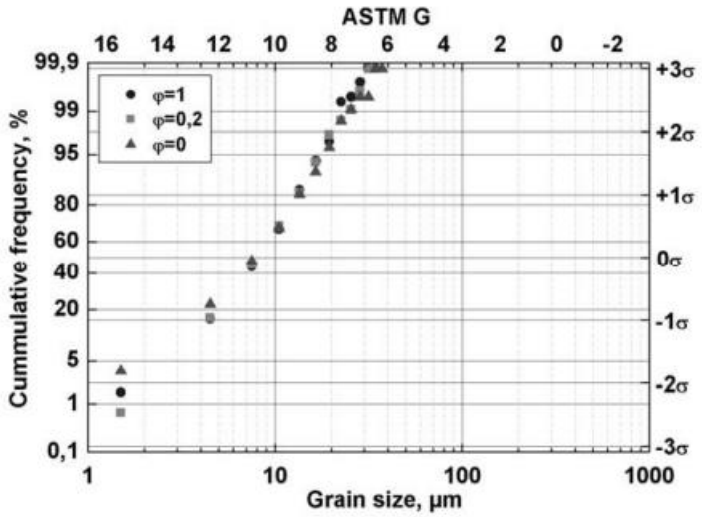

Figure 6-4 Grain size distribution of 16MnCr5+Nb steel after forging at 900°C and blank hardening at 1050°C [50]

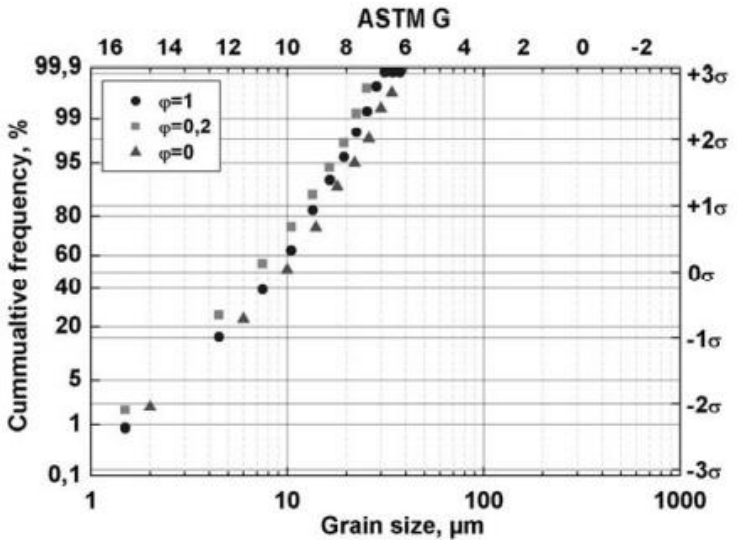

Figure 6-5Grain size distribution of 16MnCr5+Nb steel after forging at 1250°C and blank hardening at 1050°C [50]

6.4 Effect of Micro-alloying Elements on the Microstructure Evolution

Nitride and carbide precipitates: [50] Figure 6-6 shows the results of the investigated steel. In the detected temperature range of above 1000°C, the current precipitates consist mainly of AlN. Because of addition of niobium content, NbC and NbN precipitates are present. Traces of titanium lead to the small calculated quantity of TiN. With increasing the temperature, the quantity of precipitates decreases due to the lower volume fraction of precipitates. Further Ostwald ripening adds to this effect.

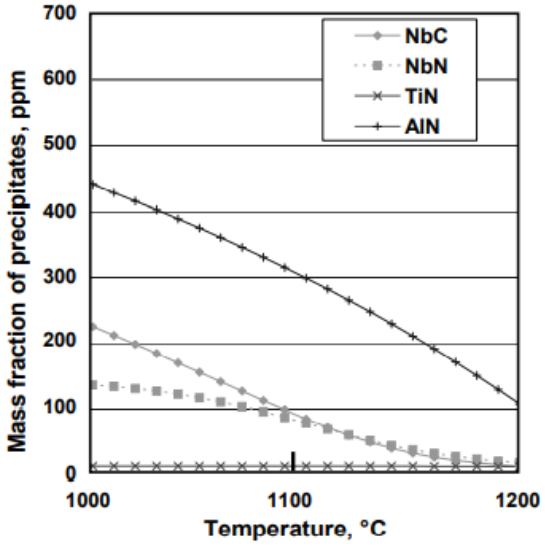

Figure 6-6 Calculated nitride and carbide precipitates [50]

Solubility and grain boundary pinning: [62] Niobium is a strong carbide and nitride former and hence, it is principally very appropriate for exerting grain boundary pinning effect by respective particles. The quantity of niobium which may be utilized for producing a suitable particle distribution depends on how much niobium may be brought into solid solution at the start of hot forming process. Therefore, steel chemistry and soaking temperature must be taken into consideration. This is a well-recognized method based on available solubility equations. Figure 6-7 shows the solubility for a steel alloy comprising 0.20% carbon and 100ppm nitrogen representing chemical composition of many typical gear steels. For characteristic soaking treatments, 0.06-0.08% niobium may be dissolved when it had precipitated as NbC after casting. Nevertheless, if it had precipitated as Nb(C,N) in the absence of a stronger nitride such as titanium, niobium's solubility is only 0.02-0.03%. other micro-alloying and alloying elements influence the solubility of niobium as well. Manganese, chromium and molybdenum in particular by their effect of lowering the activity of carbon and nitrogen increase the solubility of niobium while nickel has the opposite effect. Considering this effect in a characteristic CrMo steel chemistry, it is calculated that the solubility under soaking conditions is improved to 0.07-0.10% and 0.03-0.04% for NbC and Nb(C,N), respectively.

The same solubility curves permits approximating the quantity of niobium precipitation under carburizing conditions. Under standard carburizing temperatures (920-930°C) less than 50 ppm Nb may be in solution. For high temperature carburizing conditions, the solubility of niobium is already substantially high so that a large part of the pinning particles is lost. Hence, a larger amount must be added to the steel for sustaining a comparable particle volume fraction as under standard carburizing conditions (indicated by arrows in Figure 6-7). These solubility equations are valid for equilibrium conditions. Though, the long holding periods for soaking as well as carburizing are likely to practically meet equilibrium, at least if the particle size is not extremely large.

Particle coarsening: [62] The degree of particle ripening mechanism is controlled by the diffusivity of the particle forming species. The diffusion range of niobium in austenite is displayed in Figure 6-8. For normal carburizing temperatures, the diffusion range is restricted to around 10 µm even for very long treatment time, whereas under high-temperature carburizing conditions the diffusion range reaches values of up to 30 µm.

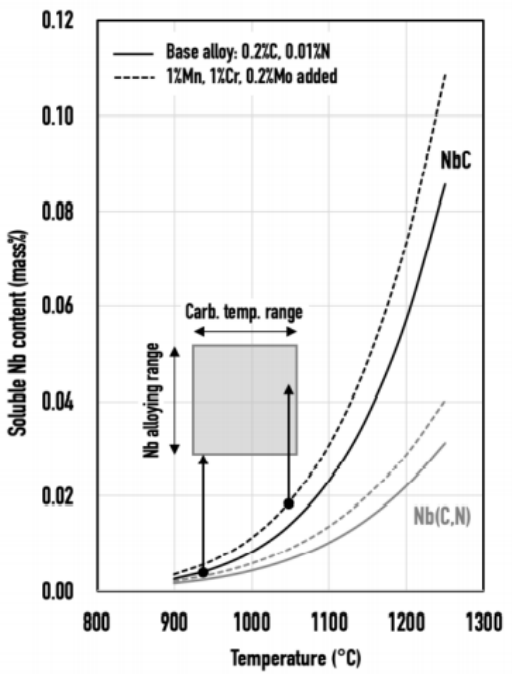

Figure 6-7 Solubility behavior of NbC and Nb(C,N) as function of temperature and influence of other alloying elements [62]

The diffusion range is a critical parameter for the growth behaviour of a particle under Ostwald ripening conditions. [63] calculated and experimentally confirmed the particle growth rate of various carbide species in austenite. Their results demonstrate that niobium carbide has a principally low growth rate being about 10^{-10} µm^3/s at 900°C and 10^{-9} µm^3/s at 1000°C.

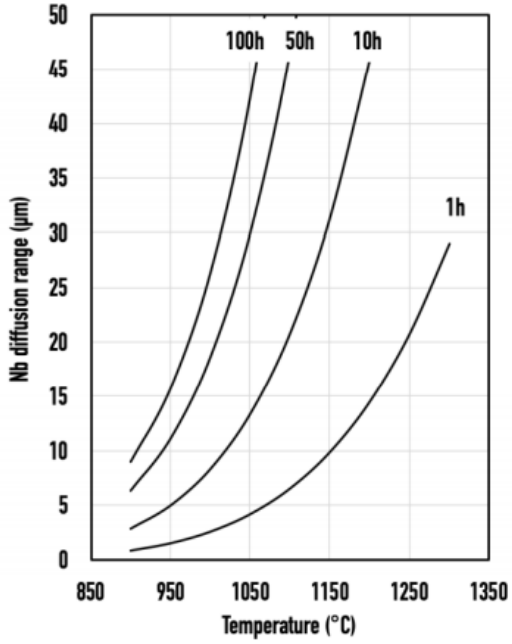

Figure 6-8 Solubility behavior of NbC and Nb(C,N) as function of temperature and influence of other alloying elements [62]

Austenite grain size control: [50] It has been recognized, that an acceptable austenite grain size control during case hardening at temperatures above 1000°C may be achieved by the application of micro-alloying elements (Nb, Ti) as well as an aligned ratio of N and Al [61]. The base steel plus Al, N and Nb shows grain size steadiness up to a simulated carburising temperature of 1075°C (Figure 6-9), depend on the combined action of Nb(C,N) and AlN. The AlN particles prevent grain growth till they become ineffective by Ostwald ripening at around 1075°C. The formation of coarse Nb nitrides at high temperature will not efficiently prevent grain growth once the AlN particles have dissolved. In contrast, fine Nb precipitates significantly decrease austenite grain growth throughout high temperature annealing. The 16MnCr5+Nb contains fine Nb(C,N) precipitates that are maximum effective in grain size stabilisation. This is demonstrated in Figure 6-9, which also shows the benefits of a joint Nb and Ti addition to the base steel composition, where fine TiN particles act as a nucleus for Nb precipitation [61]. In order to calculate and evaluate the grain coarsening effect on the mechanical properties of case hardening steels, a target area for the grain size distribution has to be well-defined. According to the routine practice of steel users the grain coarsening temperature (GCT) is related to the following limit in this investigation, all grains must be necessarily of ASTM size 5 or finer. The grains of ASTM size classes 4 and 3 are tolerated up to a total volume fraction of 10%, grains of ASTM size class 2 or coarser are not acceptable.

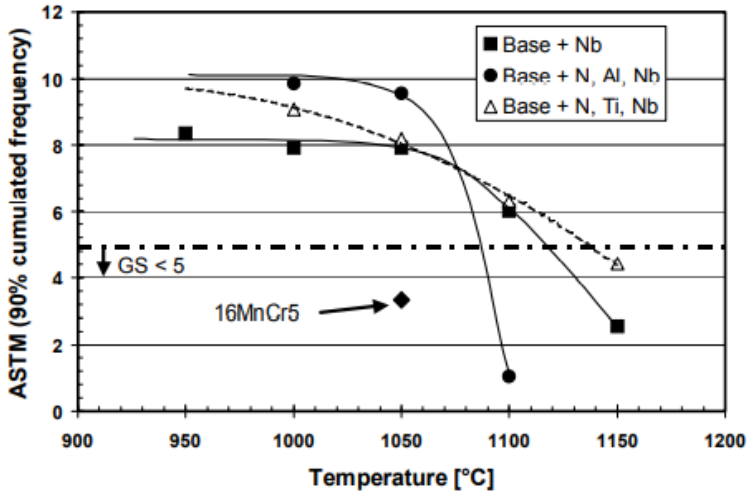

Figure 6-9 Effect of case hardening temperature on grain size. Austenizing for 2h 47min and oil quench. [50]

Fine grain stability: [64] In order to guarantee the essential fine grain stability in case hardening steels, current practice is usually to apply certain aluminium and nitrogen content in steel making process to form aluminium nitrides. Since there are additional variables that influence fine grain stability apart from the chemical composition, the manufacturing conditions as a whole must be modified to the features of the aluminium nitride dissolution and precipitation. But with this traditional material concept, grain growth still sets in at around 950 °C, which is the temperature at which the aluminium nitrides are totally in solution and can therefore no longer prevent grain growth. New kinds of micro-alloyed case hardening steels have been established in the course of the research project entitled "Carburising at temperatures above 950 °C". Additional precipitations may be formed this way by targeted addition of microalloying elements (e. g. niobium) that prevent grain growth during heat treatment up to 1050°C, and also have a significantly finer austenite grain at standard carburising temperatures. Figure 6-10 depicts the results of grain growth tests of various micro-alloyed melts based on a MoCr case hardening steel after heat treatment at 950 °C and a holding time of 25 hours in the annealed initial state. The only key difference in the chemical composition of the four melts considered is the nitrogen quantity. It is already apparent at 950 °C that the austenite grain size is turning into much finer grain as the nitrogen quantity increases, and the scatter becomes smaller.

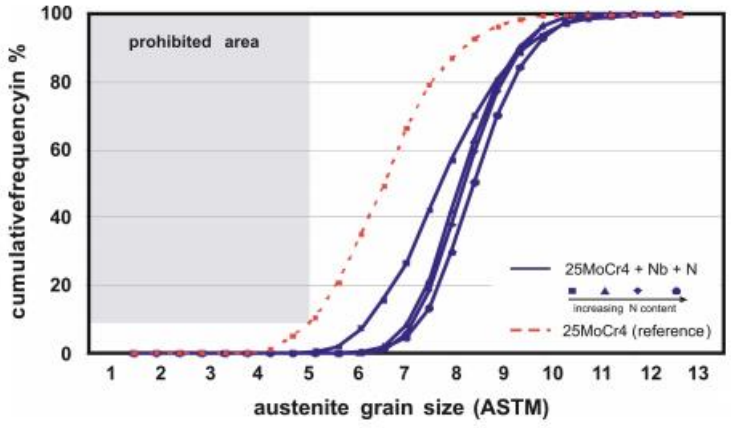

Figure 6-10 Grain growth tests of microalloyed melts of a MoCr steel in the FP annealed pre condition after 950°C and 25 hours holding time [64]

Nonetheless, about the standard carburising temperature range of 950 °C, all melts depict that the medium grain size is displaced by two grain size fractions towards finer values, as compared to the conventional reference melts. It has since been probable to show that industrial

production of micro-alloyed case hardening steels is achievable, and to transfer the findings from the laboratory trials at that time.

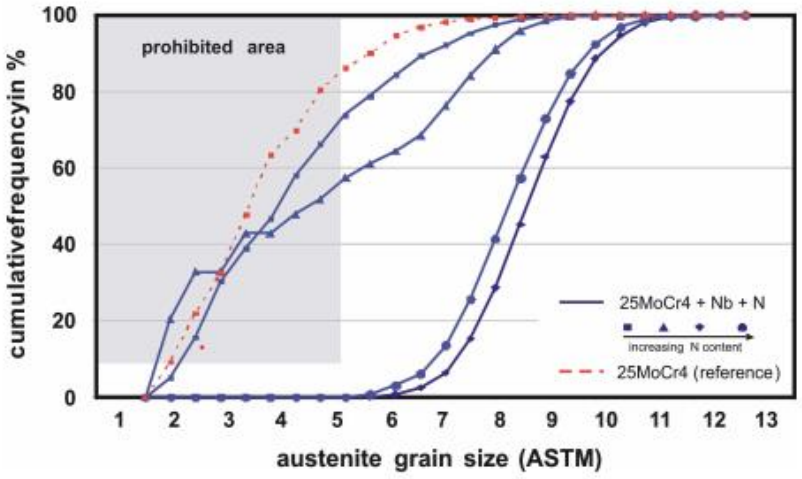

Figure 6-11Grain growth studies of the micro-alloyed melts of a MoCr steel in annealed pre-condition after 1050°C and 15 hours holding time [64]

The effect on fine grain stability of the various levels of nitrogen involved in the melts becomes clearer at higher process temperatures, where there were only two fine grain stable melts with higher nitrogen contents of around 150 ppm at 1050 °C and 15 hours, Figure 6-11.

6.5 Mechanical Properties of Niobium Micro-alloyed Steels Undergoing High Temperature Carburizing

[64] The present development potential with case hardening steels specifies that microalloying generates opportunities for the efficient use of existing and new alloys in production. Judicious adding of niobium and nitrogen in the case of molybdenum alloy case hardening steels makes a possibility of using higher process temperatures with carburizing. The grain refining effect may also or otherwise be used to even out heat treatment distortion, or to positively affect the mechanical properties of existing or recently developed materials.

Table 6-3 Mechanical properties at room temperature of 20CrMo5 mod. Steel [64]

Steel grade	Yield strength (Mpa)	Tensile strength (Mpa)	Elongation (%)
25MoCr4	727	1075	15.3
20CrMo5	772	1182	15.6
Mechanical properties according to DIN 17210:1969	Min. 700	1000-1300	Min. 8

Table 6-3 compares the mechanical properties found for the melts of 20CrMo5 modified (niobium micro-alloyed) steel and of the reference grade 25MoCr4 after blank hardening at 880° C for 2 hours, oil cooling to 180° C for 2 hours (specimen Ø 30 mm, test direction longitudinal). As anticipated, the higher hardenability of the new alloy concept is apparent in the tensile strength and yield point values. It is also apparent that in addition to the increase in strength, there can also be an increase in toughness.

7 MICRO-ALLOYING FOR HYDROGEN TRAPPING IN HIGH-STRENGTH STEELS

[65] High tensile steels are essential for weight reduction in various kinds of steel products in the steel industry. Nevertheless, as the tensile strength increases, the hydrogen-embrittlement complications become more serious. Hydrogen penetrated from the surface diffuses into the matrix of steel and collects in the strained regions and the crystallographic defects. Hydrogen creates vacancy-type defects, increases the mobility of dislocations, and/or weakens the bond of grain boundaries, which may cause fracture.

[66] To enhance the resistance to hydrogen embrittlement in high tensile steels, scattering of fine carbide precipitates such as titanium carbide (TiC), vanadium carbide (VC), niobium carbide (NbC), and their combined carbides have been proposed. These fine precipitates with high number density efficiently enhance the yield strength and tensile strength of the steels by particle strengthening mechanism, and at the same time, these precipitates act as strong trapping sites for hydrogen. Using such precipitates, it is proposed to regulate the diffusible hydrogen that directly influences the hydrogen embrittlement. To realize this, sufficient knowledge of hydrogen trapping sites and their energies in the steels is required.

7.1 Types Steels used for Micro-Alloying for Hydrogen Trapping

[67] High-strength steels with a delicate microstructure are particularly vulnerable to the effects of hydrogen embrittlement, which subsequently represents a technical restriction to the production of lighter and stronger steel structures, especially for the automotive industry. Instrumental study has been able to provide valuable data to the quality control and development of new materials, suppressing the risks of hydrogen embrittlement in steel structures. Nevertheless, merely quantitative determination of hydrogen is not sufficient to completely characterize the steel regarding its resistance against embrittlement. Thermal desorption spectrometry is a powerful tool in steel study, being able to describe hydrogen trapping sites in the microstructure, as well as the overall performance against hydrogen embrittlement. Some high-strength steels exhibit hydrogen trapping are mentioned below:

I. *0.055wt%Nb-X80 steel*: [68] Two classes of X80 steels were used in the experiment. Except for Nb, both test steels influenced the same chemical compositions, as shown in Table 7-1. Both grade steels were hot rolled at 1200ºC, and later air cooled to 830ºC for a second rolling. Instantly after rolling, test steels were water-quenched to 430~470ºC, and afterwards cooled in air to room temperature.

II. *CO80(Nb+C)*: [69] The composition of the used laboratory cast material is given in Table 7-1 and was selected for stoichiometric reasons to promote the formation of NbC precipitates. This material was manufactured in a Pfeiffer VSG100 vacuum melt and cast unit, operated in a protective argon gas atmosphere. The specimens were processed by hot and cold rolling the cast blocks to sheets with 1.7 mm thickness.

III. *NbC precipitated martensitic steel*: [70] The NbC-precipitation-strengthened martensitic steel used in this study had a niobium content of 0.05 wt.%. The steel was received in the form of 30mm thick as rolled plates. This steel was used to investigate deep hydrogen trapping in NbC/α-Fe semi-coherent interfaces. Detailed chemical composition is mentioned in Table 7-1.

Table 7-1 Chemical composition of steels [68] [69] [70]

Steel name	C	Si	Mn	P	S	Nb	Ti	Mo	Ni	Cu	N	Cr
Nb free X80	0.058	0.28	1.85	0.004	0.006	-	0.016	0.26	0.26	0.26	-	-
0.055wt% Nb X80	0.060	0.27	1.84	0.004	0.005	0.055	0.015	0.25	0.26	0.26	-	-
CO80(Nb+C)	0.013	0.0054	0.0049	-	-	0.1	0.0092	-	-	-	0.0007	-
NbC precipitated martensitic steel	0.05	-	1.10	0.007	0.002	0.05	-	-	4.50	-	-	0.53

7.2 Process Route of High-Strength Steels

CASE STUDY 1: [70]Here, the case study is discussed to explain Hydrogen trapping. The NbC precipitation reinforced martensitic steel was used in this study had a chemical composition of Fe-0.05C-1.10Mn-0.007P-0.002S-4.50Ni-0.53Cr-0.52Mo-0.05Nb wt.%. The steel was acquired as 30 mm thick rolled plates. The steel was received as 30 mm-thick as-rolled plates. These plates were sectioned into dimensions of 30×30×70 mm by electro discharge machining for additional heat treatment. Samples were austenitized at 950 °C for 30 min, and followed by water quenching to attain a full martensitic structure. These samples are referred to as-quenched steels (950-Q). To alter the size and quantity of NbC precipitates, the quenched specimens were then tempered at 440, 480, 520, and 560°C for 60 minute. The tempered specimens are referred to as Q&T-440, Q&T-480, Q&T-520, and Q&T-560, respectively. To prevent the influence of mechanical strength on HE susceptibility, a different quenching procedure (900°C for 30 min) was also studied. The corresponding as-quenched samples are denoted to as 900-Q'. A schematic representation of the heat treatment process is shown in Figure 7-1.

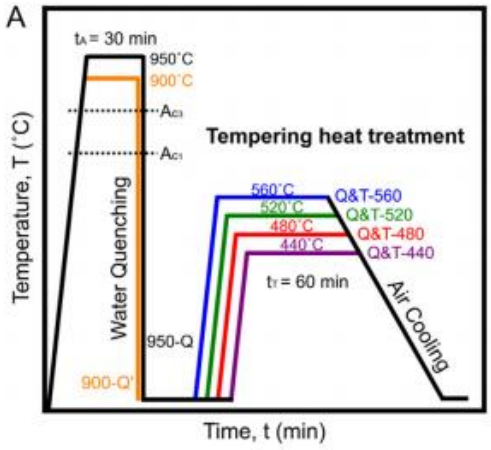

Figure 7-1 a) Schematic representation of heat treatment procedures [70]

CASE STUDY 2: [71] This case study investigates further about Hydrogen trapping. The investigational steel alloys were liquefied in a vacuum furnace and cast into ingots of 50 kg in weight. Later, the ingots were heated at 1250°C for 60 min and exposed to a treatment cycle that simulated industrial processing situations (Figure 7-2). Afterwards, hot rolling the ingots to a 3 mm gage by means of a finishing temperature of about 930°C, the hot strips were directly

transferred into an electrical furnace and kept for 60min at either 600°C or 400°C. The isothermal holding was trailed by slow cooling to room temperature after turning off the furnace. This technique simulated either a higher (600°C) or lower (400°C) coiling temperature. Consequently, the hot strips discovered a ferritic-pearlitic or bainitic microstructure, respectively. After pickling, the hot strips were cold rolled to 1.4 mm thick sheets. The cold rolled steel sheets were then heat treated using a direct current heating device, in that way simulating two possible hot stamping process variations.

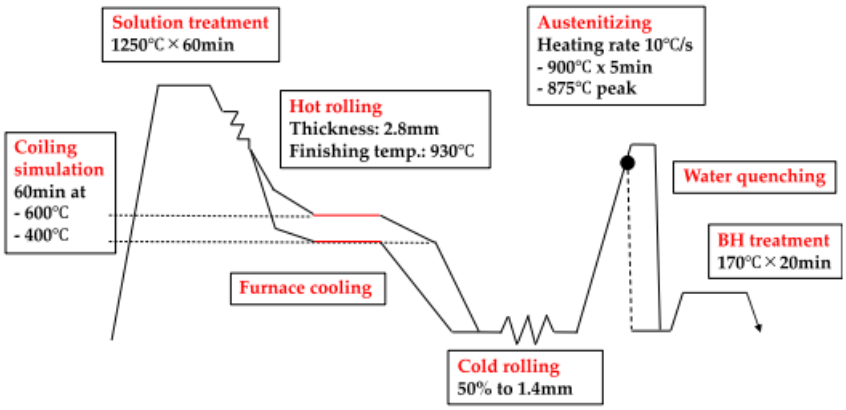

Figure 7-2 Thermo mechanical treatment schedule for production of press hardening steel [71]

In a flash heat treatment cycle ("short"), the specimens were heated with a rate of 10 °C/s to a peak temperature of 875 °C and then instantly water quenched. The traditional hot stamping cycle ("long") was replicated by soaking the steel at 900 °C for 300 s, followed by water quenching. Combinations of these processing conditions were planned to vary grain sizes and to effect the precipitation as well as the alloy segregation status. All quenched specimens were then aged at 170 °C for 20 min, simulating the paint baking cycle (bake hardening treatment) that is characteristically applied in automotive body production. Some cold rolled specimens of the base alloy were also austenitized at higher temperatures (1000–1200 °C) in order to provoke coarser austenite grain sizes.

It is important to note that the conditioning of the material and the associated test results originating from this study represent the steel performance during the vehicle use phase. Many published results on the hydrogen embrittlement of PHS, on the contrary, refer to the as-quenched state, i.e., formerly the bake hardening treatment. Such results obtained in the as-quenched condition signify the intermediate phase, between the press shop and final assembly.

7.3 Microstructure Evolution- Hydrogen Embrittlement and Hydrogen Trapping

7.3.1 Fundamentals of Hydrogen Embrittlement

[72] Hydrogen in iron is an important and intensively examined subject, because several severe failure cases may be caused by hydrogen embrittlement of steels.

From the atmosphere, afterwards adsorption and dissociation, hydrogen is dissolved by absorption according to:

$$H_2(gas) = 2H\ (dissolved)$$

Equation 9

And its concentration is followed by Sieverts law:

$$c_H = K_s.(PH_2)^{\frac{1}{2}}$$

Equation 10

Here, c_H is in mol/cm^3 is the concentration of dissolved H atom, K_s is Sieverts constant and PH_2 is in bar the hydrogen pressure in environment. In α-Fe that corresponds to 3 cm^3 H_2/100g, the solubility at 1 bar pressure and room temperature is 3 x 10^{-6} %, is tremendously low and rises to about 1.6 x 10^{-2} % at 900ºC. In the case of γ-Fe, the solubility is a little higher and is 2.3 x 10^{-2} % at 900ºC and in the melt c_H is much higher at 0.13 % at 1540ºC. So it is unsafe to saturate steels at elevated temperatures with H and cool down with the possibility for H_2 desorption, that may be hindered by oxide scales or zinc coatings, an over saturated solution results that causes some failures like shatter cracks, flakes, fish eyes etc.

Hydrogen absorption happens not only from atmospheres but more frequently from electrolytes, example during pickling or by corrosion of steels. Some of the most important reactions during corrosion of iron in an acid environment are:

$$Fe + 2\,H^+ = Fe^{2+} + 2H_{ad}$$

Equation 11Anodic dissolution of Fe (Volmer reaction)

$$2\,H_{ad} = H_2(gas)$$

Equation 12 Recombination of absorbed H (Tafel reaction)

$$H_{ad} = H(dissolved)$$

Equation 13: Absorption of H_{ad}

The interplay of these reactions creates a hydrogen activity on the metal surface that is strongly affected by inhibitors and promoters in the electrolyte and by the presence of alloying elements and impurities in the metal surface. The hydrogen activity is well-defined as the hydrogen concentration c_H related to the hydrogen concentration c_H^0 at temperature of 0ºC and 1 bar hydrogen pressure. If the anodic dissolution reaction Equation 11 is improved (by the presence of sulphur) and/or the recombination reaction Equation 12 is retarded (example by arsenate) very high hydrogen activities may occur on steel surfaces that cause severe absorption of hydrogen.

Hydrogen is very hazardous, especially in ferritic steels since it usually diffuses very fast to the defects, where it exerts its deleterious actions. As a matter of fact, the diffusivity of H in pure and under-formed α-iron at room temperature is very high.

7.3.2 Hydrogen Trapping

[1] Niobium is known act as hydrogen trapping element. The mechanism by which niobium enhances delayed fracture resistance in steels is unknown at the moment. But there are two main proposals related to this:

I. Niobium/carbon act as a hydrogen trap- main mechanism.

II. The grain refinement effect of niobium (C,N)- secondary mechanism.

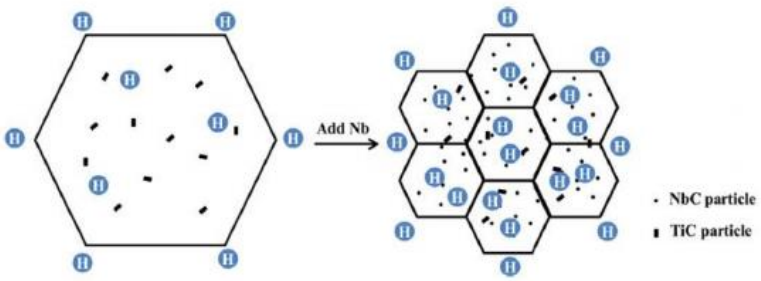

Figure 7-3 Hydrogen trapping by the addition of Niobium [1]

Hydrogen Induced Crack:

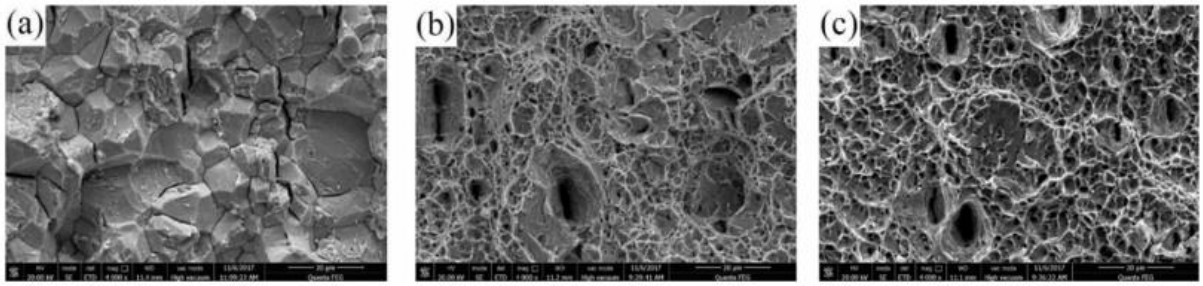

Figure 7-4 Fracture surfaces for the specimens with different content of Nb, a) 22MnB5, b) 22MnB5 + 0.027%Nb, c) 22MnB5 + 0.049%Nb [73]

[73] Figure 7-4 depicts the engineering stress vs strain curves gained from specimens. It may be seen that delayed fracture resistance of press hardening steel charged electrochemically increases with the niobium addition (Press hardening steel (PHS): PHS-3 > PHS-2 > PHS-1). When the rate of strain is 1 x 10^{-5} s^{-1} , the present density is 10mA/cm^2 , the critical fracture stress of tested steel for slow strain rate test (SSRT) is around 520MPa, 720MPa and 1150MPa respectively. It is worth noting at this point that for the tests of PHS-1 and PHS-2 specimens, the effect of strain on tensile properties is not significant at strain levels of 0-4.5%, whereas the strain becomes noticeable when strain exceeds 4.5%. When compared with PHS-1 and PHS-2 samples, the influence of the strain in tensile properties of PHS-3 and sample is obviously greater than that at the same strain.

In a nutshell, the hydrogen induced cracking resistance of press hardening steel can be improved significantly by the addition of niobium. Furthermore, the effect of niobium on hydrogen induced cracking of high strength hot stamping steel is explained in Figure 7-4. Apparently, the fractography of niobium free specimen exhibits characteristic brittle intergranular fracture (Figure 7-4 (a)). Also, Figure 7-4 (b) shows the fracture surface of specimen containing 0.27% of niobium is the mix feature of quasi-cleavage fracture and ductile fracture. Interestingly, when the content of niobium is 0.049% in PHS 22MnB5, the fracture appearance reveals obvious dimple fracture, and the dimple is deeper and bigger with the increase of niobium. This indicates that the addition of niobium element in press hardening steel 22MnB5 significantly improves the resistance of hydrogen induced fracture and takes the transition of intergranular fracture to dimples. This is the reason why the nanoscale precipitates of Nb(C,N) are formed in the micro-structure samples and act as hydrogen trap and pinch

hydrogen atoms, that reduce the susceptibility of hot stamped steel of hydrogen embrittlement, and ultimately leads to the increase in tensile strength and elongation of PHS samples with increase in niobium concentration in SSRT. As a result, the results of the fractography for the specimens after the SSRT with different content of niobium is consistent well with the critical fracture strength of tested steels for SSRT.

Effect of Precipitates on the Hydrogen Induced Cracking:

[73] When the material is under the state of continuous load with hydrogen, the hydrogen would rather gather near the micro-cracks acted as hydrogen trappings, then the hydrogen pressure was created and the stress at the crack tips would increase finally. Generally, the micro-cracks expanded along the cleavage plan when the stress is high enough.

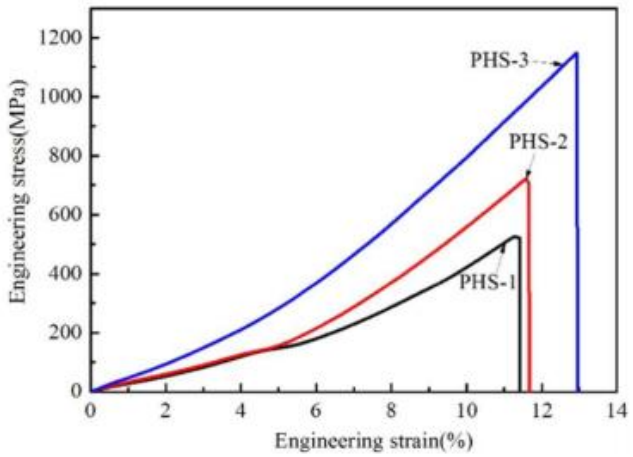

Figure 7-5 Stress-Strain curves of tested steels electrochemically charged at various contents of Nb [73]

The grain boundaries and large sized precipitates are generally major hydrogen trapping sites in press hardening steel 22MnB5, hence, hydrogen induced delayed micro-cracks preferentially nucleate at these sites, then propagate under the combined action of hydrogen and the applied stress. The precipitates Nb(C,N) are reported to be active sites to trap hydrogen and importantly determine the hydrogen induced cracking process. Thereinto, hydrogen diffused faster into grain boundaries than into austenite lattice. This is the indication that the lath boundaries of martensite effectively hindered the propagation of cracks. A large number of researchers have established hydrogen trapping performance of micro-alloy precipitates. [74] The capacity of hydrogen trapping in coherent micro-alloy carbides varies in the descending order of NbC > TiC > VC. The precipitates of Nb(C,N) particles are occurring at significantly lower

temperature and much smaller in size than TiN, moreover, they allow a uniform distribution of hydrogen. This mostly reflects the fact that the nano-particles strongly interact with hydrogen and have high escape activation energy that is necessary for hydrogen to leave particles, Nb(C,N) belongs to this hydrogen trapping. From Figure 7-5, the improvement of hydrogen induced fracture resistance is achieved by the precipitates of Nb(C,N).

Generally, there are two purposes of alloy design in the enhancement of hydrogen induced cracking resistance. One is to control the boundary characteristics of the PHS, and the other is to intensify the nucleation positions of the hydrogen trapping. Austenite grain may be refined by the addition of niobium element, that will contribute to improve the hydrogen induced delayed fracture due to the enhancement of intergranular strengthening. It is very effective of niobium in hydrogen embrittlement to promote a fine and uniform distribution of carbonitrides.

7.4 Effect of Niobium Micro-alloy on Hydrogen Trapping

[73] The microstructure, mechanical properties and hydrogen induced cracking of PHS 22MnB5 containing various amount of niobium were investigated. Although 22MnB5 is not used in powertrain due to low hardenability, the steel is investigated in this thesis to understand hydrogen induced cracking. With the purpose of comprehending the influence of niobium precipitation behaviour on above discussed aspects. As a result, following effects of niobium addition as a micro-alloy were obtained:

I. The microstructure of PHS 22MnB5 containing niobium are finer than that of steel without niobium. Moreover, the lath martensite is narrower with the increase of niobium content because of the precipitates Nb(C,N) that increases with the addition of niobium element.

II. The hydrogen trapping presentation of hot forming 22MnB5 steel gets a significant optimization potential owing to the increase of the precipitates Nb(C,N), that indicates the hydrogen embrittlement resistance of 22MnB5 may be improved remarkably by increasing niobium content.

III. Fracture analysis of 22MnB5 surfaces after hydrogen charging at same current density discloses an increase in ductile dimple type pattern with the addition of niobium , that is the hydrogen trapping impact of dispersed Nb(C,N) nanoparticles.

7.5 Mechanical Properties of Niobium Micro-Alloyed Steels after undergoing Hydrogen Trapping Effect

Because of combing the forming and quenching process, hot stamping may obtain the full martensitic microstructure to tremendously enhance the strength of press hardening steels.

Figure 7-6 shows the engineering stress-strain curves of the PHS, the Table 7-1depicts the mechanical properties of the specimens. It may be seen that the tensile strength of hot rolled steel is about 850-950 MPa and the elongation is over 14%, but the ultimate tensile strength (UTS) is over 1600MPa and the elongation (EL) is 13-14% after hot stamping.

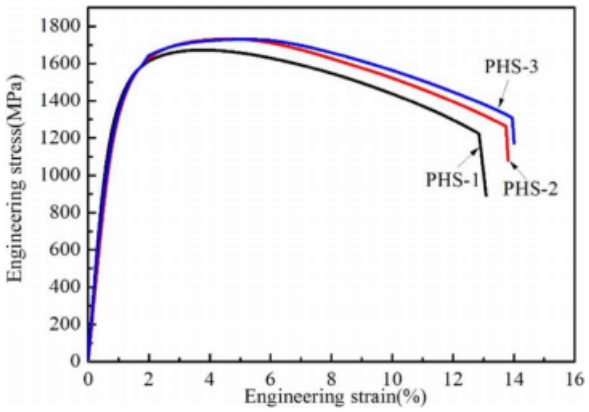

Figure 7-6 Engineering stress vs strain curves of the three PHS [73]

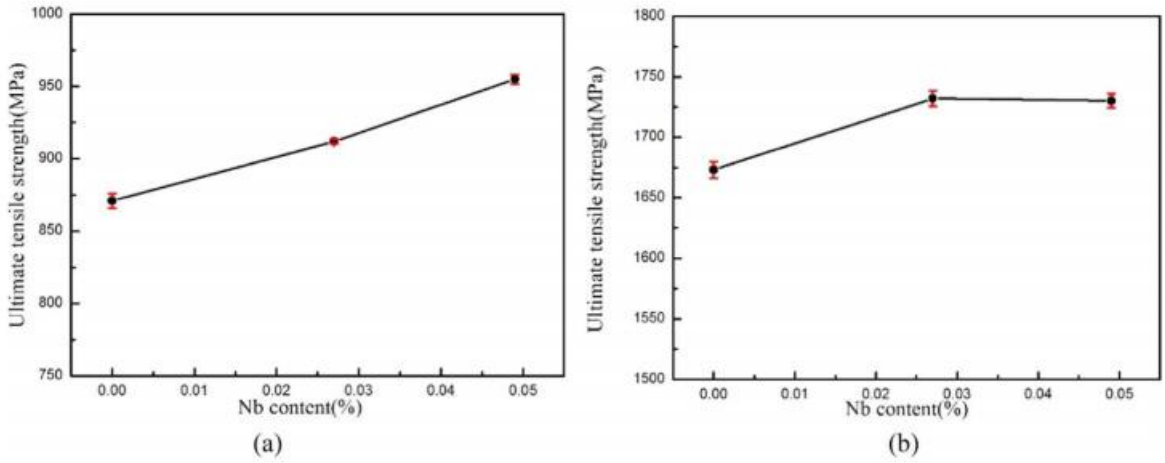

Figure 7-7 Tensile strength of investigated steel with various niobium content a) hot rolled steels b) press hardening steels [73]

Table 7-2 Tensile properties of investigated steels [73]

Materials	Hot Rolled Steels			Press Hardening Steels		
	YS (MPa)	UTS (MPa)	EL (%)	YS (MPa)	UTS (MPa)	EL (%)
1	587	871	14.76	1288	1673	13.09
2	613	912	15.76	1339	1732	13.82
3	508	955	16.60	1269	1730	14.00

The hot stamping process has been raised two times in the UTS as hot rolled and has a slight decline in the elongation. To the various alloy steels, the UTS and EL are slightly different, and this may be that the microstructure is not exactly the same. An error bar of the tensile strength values for Table 7-2 is shown in Figure 7-7, where the black dots signify the average and the red bars signify the maximum and minimum of the two measures. It may be seen from the graph that the tensile strength of hot rolled steels rises with the addition of niobium content,. And the tensile strength if press hardening steels first increases with the addition of niobium, and then finally maintains ar 1730MPa or so.

8 Conclusion

This thesis aimed to investigate the role of niobium in the automotive steels, particularly for powertrain and transmission systems. In order to accomplish a useful weight reduction from an environmental point of view, essential in the last years, niobium signifies a good strategy. The element was discovered in 1801 and currently its production is predominantly performed by CBMM, a Brazilian society that over the year has implemented increasing extraction technology, and makes it possible a continuous development in its research and applications.

Throughout the research it has been found that a small addition of Nb has great effect on steel, for example an amount of 0,01% Nb in hot rolling could increase the mechanical properties even by 25%. Mechanisms by which it acts are mainly three:

I. Grain refinement: This is the most significant effect because it allows an enhancement of both strength and elongation. It works over the solute drag of the atoms in solid solution and the pinning force exerted by precipitates. Thanks to grain refinement it's probable to obtain a pancaked structure during hot rolling, in which grain are elongated. Meanwhile the recrystallization process is delayed, fragmentation of this elongated grains leads to new smaller ferritic grains.
Finer microstructure strengthens materials thorough the Hall-Petch mechanism, and at the same time makes fracture propagation more difficult, since the cracks has to follow a longer pathway.

II. Precipitation: The analysis of solubility products and application of an enhanced controlled process result in an efficient precipitation, which causes grain refinement and give a strengthening contribute. It varies on size and shape of the particles, in fact their significances have been presented in some scientific reached reported in the discussion. Precipitation occurs through the various phases of steel production, and its outputs are affected by situation in which they are formed. For example the shape of early precipitates might different from the others due to the interaction with Ti particles that are added stable at high temperatures. On the other hand, as an alternative, NbC (the main niobium precipitates) formed in the ferritic region or during coiling are finer and their possibility of coarsening is reduced for the shorter time at lower diffusivity condition. Combination with different element

(microalloying or others) has been examined, together with comparison of the several standings.

III. Prevention of hydrogen embrittlement: This phenomenon appears particularly in the high-strength steels, that are subjected to a more brittle behaviour. Hydrogen accumulation is the cause of delayed fractures that are deleterious for a precise fatigue resistance. Niobium is advantageous for this aspect because it acts as a hydrogen trap, so a more uniform and distributed dispersion it's attainable. In this way, hydrogen accumulation is avoided and ductility is increased.
It has also been seen that niobium encourages other microstructural implications (such as more low angles grain boundaries) that help embrittlement resistance.

In chapter 3, it was carried out an investigation on the principal typologies of steels used in automobile construction. Niobium effects on the various classes are more or less the same, but in each type single feature is more or less pronounced in comparison to another one. In very high-strength martensitic steel microstructural refinement is, yet again, the finest niobium effect, because in these steels there is no request of strengthening, but elongation. Reduced grains arising from niobium allow to gain some fraction of attainable strain, so ductility is increased. In ultra-low carbon steel, as an alternative, the essential feature is the formability. Therefore, the importance of niobium lies in regulation of the interstitial atoms (mainly C and N) in order to satisfy the requirement of ductility and strength (if necessary).

Consequently, it can be concluded that in a perception of growing enhancements that distinguishes the contemporary age, niobium play a prominent role in a lot of applications, particularly in the automotive field, where a very large fraction of the steel is micro-alloyed with niobium.

9 References

[1] F. D'Auito and J. Bolota, “Introduction to Niobium improving the performance of SBQ engineering steels,” 2020.

[2] A. Tina, “Niobium micro-alloyed steels for automotive applications,” 2020.

[3] J. ECKERT, S. Hermann, W. Goslar, Goslar and Federal republic of Germany, “Niobium and Niobium compounds”.

[4] G. Genta, L. Morello, F. Cavallino and L. Filtri, The motor car- Past, present and furute, Springer, 2014.

[5] P. Mallick, “Advanced materials for automotive applications: An overview,” *Advanced materials in automotive engineering,* pp. 5-27, 2012.

[6] E.V.Sidorov, “Equilibrium Phase Diagram of the Iron-Carbon System,” *Izvestiya VUZ Chernaya Metallurgiya,* vol. 38, no. 11, pp. 3-5, 2008.

[7] W. Callister and D. Rethwisch, Material Science and Engineering, Wiley India Pvt. Ltd., 2014.

[8] S. Ahmad, “Presence of golden ratio relationships in Fe-Fe3C, Cu-Zn and Cu-Sn alloy systems,” *International journal of design and nature and ecodynamics,* vol. 10, pp. 174-181, 2015.

[9] R. V, “C-Fe-Nb (Carbon-Iron-Niobium),” *Journal of Phase Equilibria,* vol. 24, 2003.

[10] H. Ohtani, M. Hasebe and T. Nishizawa, “Calculation of the Fe-C-Nb Ternary Phase Diagram,” *CALPHAD,* vol. 2, no. 13, pp. 183-204, 1989.

[11] W. Huang, “A Thermodynamic Evaluation of the Fe-Nb-C System,” *Z. Metallkd,* vol. 6, no. 81, pp. 397-404, 1990.

[12] v. G. O.K., “Springer,” Springer, Berlin, Heidelberg, 1982. [Online]. Available: https://link.springer.com/chapter/10.1007%2F978-3-662-08024-5_42#citeas.

[13] K. Balasubramanian, A. Kroupa and J. Kirkaldy, “Experimental Investigation of the Thermodynamics of Fe-Nb-C Austenite and Non-stoichiometric Niobium and Titanium Carbides (T=1273 to 1473K),” *Metall. Trans.,* vol. 23A, pp. 729-44, 1992.

[14] V.K.Lakshmanan and J. Kirkaldy, “Solubility Product for Niobium Carbide in Austenite,” *Metall. Trans. ,* no. 15A, pp. 541-544, 1984.

[15] R.C.Das, R. Jha and T. Mukharjee, “The Carbon-Iron-Niobium System,” *Journal alloy phase diagrams,* vol. 2, no. 2, pp. 131-140, 1986.

[16] H. Ohtani, T. Nishizawa, T. Tanaka and M. Hasebe, “Proceedings of Japan Canada seminar on Secondary steel-making,” *The Canadian Steel Industry ASsociation and the Iron and the Steel Institute of Japan,* pp. J-7-1 to J-7-12, 1985.

[17] S. Jonsson, “Assessment of the Fe-Ti-C system, Calculation of the Fe-Ti-N System, and Prediction of Solubility Limit of Ti(C,N) in Liquid Fe,” *Metall. Mater. Trans. B,* no. 29B, pp. 371-84, 1998.

[18] G. Krauss, Steels- Processing, Structure, and Performance, Ohio: ASM International, 2015.

[19] E. Turkdogam, “Causes and Effects of Nitride and Carbonitride Precipitation during Continuous Casting,” *Iron Steelmaker,* vol. 16, pp. 61-75, 1989.

[20] P. Repas, “Metallurgical Fundamentals for HSLA Steels,” *ASM International,* pp. 3-14, 1988.

[21] L. Cuddy and J. Raley, “Austenite Grain Coarsening in Microalloyed Steels,” *Metall. Trans.,* vol. 14, pp. 1989-1995, 1983.

[22] F. Perrard, P. Donnadieu, A. Deschamps and P. Barges, “TEM Study of NbC Heterogeneous Precipitaion in Ferrite,” *Philosophical Magazine,* vol. 86, no. 27, pp. 4271-4284, 2006.

[23] C. Klinkenberg, K. Hulka and W. Bleck, “Niobium Carbide Precipitaion in Microalloyed Steel,” *Steel Research,* no. 11, pp. 744-758, 2004.

[24] Y.-S. Chen, h. Lu, J. Liang, A. Rosenthal, H. Liu, G. Sneddon, I. McCarroll, Z. Zhao, W. Li, A. Guo and J. M. Cairney, “Observation of Hydrogen Trapping at Dislocations, Grain Boundaries, and Precipitates,” *Science,* vol. 367, no. 6474, pp. 171-175, 2020.

[25] E. Wallaert, T. Devopar, B. Pieters, M. Arafin and K. Verbeken, “TDS evaluation of the hydrogen trapping capapcity of NbC precipitates,” *International Hydrogen Conference ,* pp. 575-584, 2012.

[26] Gehrmann, “The effect of the nitrides and carbides of V, Nb, and Ti on the diffusion and dissolution of hydrogen in iron,” *Hydrogen transport and cracking in metals,* pp. 216-226, 1995.

[27] P. Subramanyam, A. A. A. Guzman, S. Vincent, A. Hartmaier and R. Janisch, “Ab initio study of combined effects of alloying elements and H on grain boundary cohesion in ferritic steels,” *Metals,* vol. 9, no. 3, p. 291, 2019.

[28] De Backer, D. Mason, C. Domain, D. Nguyen-Manh, M. Marinica, L. Ventelon, C. Becquart and S. Dudarev, “Multiscale modelling of the interaction of hydrogen with interstitial defects and dislocations in BCC tungsten,” *Nuclear Fusion,* vol. 58, no. 1, p. 016006, 2018.

[29] M. P.K, “Advanced materials for automotive applications: an overview,” *Advanced materials for automotive engineering,* pp. 5-27, 2012.

[30] Q. Li, L. Xie, J. Song, H. Li and G. Xu, “Research Methods and Applications of Gear Manufacturing Process Optimization,” *Mathematical problems in Eengineering,* pp. 1-17, 28 May 2019.

[31] K. Sirang, “Determination of the Number of Kanban for Automotive Axle Production,” *IEEE 7th International Conference on Industrial Engineering and Applications (ICIEA),* pp. 20-24, 2020.

[32] H. Zainul, “Reengineering of heat-treatment system for axle-shaft of racing cars,” *Materials and design,* vol. 6, no. 26, pp. 561-565, 2005.

[33] K. HS, J. Kim and J. Kim, “Design and manufacture of an automotive hybrid aluminum/composite drive shaft,” *Composite structures,* vol. 1, no. 63, pp. 87-99, 2004.

[34] A. Farshidianfar, M. Ebrahimi, H. Rahnejat, M. Menday and M. Moavenian, “Optimization of the high-frequency torsional vibration of vehicle driveline systems using genetic algorithms.,” *Journal of Multi-body Dynamics,* vol. 3, no. 216, pp. 249-262, 2002.

[35] D. Cho and J. Choi, “Manufacture of one-piece automotive drive shafts with aluminum and composite materials,” *Composite structures,* vol. 38, no. 1-4, pp. 309-319, 1997.

[36] F. Schmelz, H. Seherr-Thoss and E. Aucktor, “Universal joints and driveshafts: analysis, design, applications.,” in *Springer-Verlag*, New York, 1992.

[37] M. Lee, S. Kim, H. Han and W. Jeong, "Application of hot press forming process to manufacture an automotive part and its finite element analysis considering phase transformation plasticity," *International Journal of Mechanical Sciences,* vol. 11, no. 51, pp. 888-898, 2009.

[38] S. P, H. Adrian and J. Sinczak, "Controlled cooling of drop forged microalloyed-steel automotive crankshaft," *Archives of Metallurgy and Materials,* vol. 56, no. 1, pp. 93-107, 2011.

[39] S. Sankaran, S. Sangal and K. Padmanabhan , "Microstructural evolution and tensile behaviour of medium carbon microalloyed steel processed through two thermomechanical routes," *Materials science and technology,* vol. 21, no. 10, pp. 1152-1160, 2005.

[40] J. Zrnik, T. Kvackaj, A. Pongpaybul, P. Sricharoenchai, J. Vilk and V. Vrchrovinsky, "Effect of thermomechanical processing on the microstructure and mechanical properties of Nb–Ti microalloyed steel," *Material science and engineering,* vol. 319, pp. 321-325, 2001.

[41] D. Nakhaie, P. Benhangi, F. Fazeli, M. Mazinani, E. Karimi and M. Ferdowsi, "Controlled forging of a Nb containing microalloyed steel for automotive applications," *Metallurgical and Materials Transactions,* vol. 43, no. 13, pp. 5209-5217, 2012.

[42] V. Ryan, "Design and Technology AND Engineering," 2020. [Online]. Available: https://technologystudent.com/despro2/forging21.html.

[43] S. S, N. Ramisetti, R. Misra, T. Mannering, D. Panda and S. Jansto, "Effect of cooling rate on the microstructure and mechanical properties of Nb-microalloyed steels.," *Materials Science and Engineering: A,* no. 460, pp. 335-43, 2007.

[44] J. Hannula , D. Porter, A. Kaijalainen, M. Somani and J. Komi, "Optimization of Niobium Content in Direct Quenched High-Strength Steels," *Metals,* vol. 10, no. 6, p. 807, 2020.

[45] A. Kaijalainen, P. Suikkanen, T. Limnell, L. Karjalainen, J. Komi and D. Porter, "Effect of austenite grain structure on the strength and toughness of direct-quenched martensite.," *Alloy Compound,* vol. 577, pp. S642-S648, 2013.

[46] T. Maccagno, J. Jonas, S. Yue, B. McCrady, R. Slobodian and D. Deeks, "Determination of Recrystallization stop temperature from rolling mill logs and comparison with laboratory simulation results," *ISIJ international,* vol. 34, no. 11, pp. 917-922, 1994.

[47] C. Fossaert, G. Rees, T. Maurickx and H. Bhadeshia, "The effect of niobium on the hardenability of microalloyed austenite," *Metallurgical and Materials Transactions A,* vol. 26, no. 1, pp. 21-30, 1995.

[48] K. Toshimitsu and Y. Kurebayashi, "Niobium in microalloyed engineering steels, wire rods and case carburized products.," *International Symposium on Niobium,* pp. 801-819, 2001.

[49] N. V, "Application of niobium microalloying in heat treatment of engineering steels," *International Heat Treatment and Surface Engineering,* vol. 8, no. 2, pp. 80-85, 2013.

[50] S. Trute, W. Bleck and C. Klinkenberg, "Advanced Material and Process Development for Steels for Automotive Applications," *New Developments in Long and Forged Products Proceedings,* pp. 161-168, 2006.

[51] W. Bleck and F. Hippenstiel, "Microalloying in case hardening steels," *Proc. HSLA steels,* pp. 98-104, 2000.

[52] H. Mohrbacher, "Reverse metallurgical engineering towards sustainable manufacturing of vehicles using Nb and Mo alloyed high performance steels," *Advaned manufacturing,* vol. 1, pp. 28-31, 2013.

[53] D. K. Matlock, J. G. Speer, S. G. Jansto and M. Stuart, "Microalloyed Steels for Heat Treating Applications at Higher Process Temperatures," *Journal of Iron and Steel Research, International,* vol. 18, no. 1, 2011.

[54] D. K. Matlock, J. G. Speer, S. G. Jansto and M. Staurt , "Development of Microalloyed Steels for High Temperature carburizing," in *Proceedings of the Fourth Baosteel Biennial Academic Conference*, Shanghai, China, 2010.

[55] R. Galdino, J. De Paula, C. Coromberk, J. Pinto, M. De Almeida and S. Freese, "An application of Nb-Ti microalloying for carburizing steels," Sao Paulo, Brazil.

[56] R. Thompson, D. Matlock and J. Speer, "The fatigue performance of high temperature vacuum carburized Nb modified 8620 steel," *SAE Transactions,* pp. 392-407, 2007.

[57] T. T, F. Hippenstiel and H. Mohrbacher, "Optimizing gear performance by alloy modification of carburizing steels," *Metals,* vol. 7, no. 10, p. 415, 2017.

[58] S. Trute, W. Bleck and C. Klinkenberg, "Advanced material and processing for the high temperature carburising of microalloyed case hardening steels," *Materials Science Forum,* vol. 539, pp. 4470-4475, 2007.

[59] T. S, Bleck W, F. Hippenstiel and C. Klinkenberg , “Microalloying in case hardening steels – a challenge for the lean production of gears,” in *Int.. Conf. on Steels in Cars and Trucks*, Wiesbaden, Germany, 2005.

[60] S. Hock, J. Kleff, I. Kellermann and M. Schulz , “Temperature - the key to optimize cost and result in carburizing vehicle driveline parts,” in *; Int. Conf. Steels in Cars and Trucks*, Wiesbaden, Germany, 2005.

[61] W. Bleck , G. Pariser, S. Trute and C. Klinkenberg, “New Developments for Microalloyed Heat Treating Steels, Proceedings of THERMEC,” *, Processing and Manufacturing of Advanced Materials,* Vols. 426-432, no. 2, pp. 1201-1206, 2003.

[62] H. Mohrbacher, “Alloy design and processing strategies for grain coarsening-resistant carburizing steels,” Schilde, Belgium.

[63] W. M.Y, T. Sakuma and T. Nishizawa, “Growth of Alloy Carbide Particles in Austenite,” *Transactions of the Japan Institute of Metals,* vol. 22, no. 10, pp. 733-742, 1981.

[64] H. F, “Improvement Working and Utility Properties of Classical and New Mo-alloyed Carburizing Steels,” in *3rd International sCT Conference steels for Cars and Trucks. 2011.*, Wetzlar, Germany, 2011.

[65] T. J, K. Kawakami and Y. Kobayashi, “Origin of hydrogen trapping site in vanadium carbide precipitation strengthening steel,” *Acta Materialia,* vol. 153, pp. 193-204, 2018.

[66] G. Pressouyre, “A classification of hydrogen traps in steel,” *Metall Trans.,* vol. 10, pp. 1571-73, 1979.

[67] K. Bergers, E. Casimao de Souza, I. Thomas, N. Mabho and J. Flock, “Determination of Hydrogen in Steei by Thermai Desorption Mass Spectrometry,” *steel research Int. ,* vol. 81, no. 7, pp. 499-508, 2010.

[68] C. Q, J. Wu, D. Xie, X. Wu, Y. Huang and X. Li, “Effect of nanosized NbC precipitates on hydrogen diffusion in X80 pipeline steel. Materials,” *Materials ,* vol. 10, no. 7, p. 721, 2017.

[69] E. Wallaert, T. Depover, B. Pieters, M. Arafin and K. Verbeken, “TDS evaluation of the hydrogen trapping capacity of NbC precipitates.,” *International Hydrogen Conference,* pp. 575-584, 2012.

[70] S. Rongjian, M. Yuan, W. Zidong, G. Lei, Y. Xu-Sheng and Q. Lijie, "Atomic-scale investigation of deep hydrogen trapping in NbC/α-Fe," *Acta Materialia,* vol. 200, pp. 686-698, 2020.

[71] H. Mohrbacher and T. Senuma , "Alloy optimization for reducing delayed fracture sensitivity of 2000 MPa press hardening steel," *Metals,* vol. 10, no. 7, p. 853, 2020.

[72] H. Grabke, F. Gehrmann and E. Riecke, "Hydrogen in microalloyed steels," *Steel research,* vol. 72, no. 5-6, pp. 225-235, 2001.

[73] L. Lin, L. Bao-Shun, Z. Guo-ming, K. Yong-lin and L. Ren-dong, "Effect of Niobium precipitaiton behaviour on microstructure and hydrogen induced cracking of press hardening steel 22MnB5," *Material science and engineering A,* vol. 721, pp. 38-46, 2018.

[74] F. Wei, T. Hara and K. Tsuzaki, "Nano-precipitates design with hydrogen trapping character in high strength steel," *Adv. steels,* pp. 87-92, 2011.

[75] J. Hannula, D. Porter, A. Kaijalainen, M. Somani and J. Komi, "Optimization of Niobium Content in Direct Quenched High-Strength Steels," *Metals,* vol. 10, no. 6, p. 807, 2020.